PARTICLE WORLD

Technical Papers of QUANTACHROME

Edition 5 • September 2012

Application notes – download the complete list from www.quantachrome.eu.com

New: Particle size and shape analysis from 0.2 µm up to 3 cm

POROMETER 3G series - Characterization of filters, membranes, papers, nonwovens...

Review-article -
Determination of specific surfaces (BET surface area) of different dimensions

Dear Reader,

new implemented methods and new developed instruments for the characterization of dispersions, powders and porous solids are the basis of the great success of QUANTACHROME in the field of the comprehensive particle characterization. With the patented TURBISCAN (Lab, On-line and automated AGS version) one can characterize the stability of original dispersions by use of both transmitted and backscattered light. Further in the field of **characterization of dispersions** we offer the RHEOLASER Lab for the unique determination of µ-rheological properties of soft materials as emulsions, suspensions, gels or polymers.

Recent developments in the field of **characterization of porous solids** are related to the gas adsorption instruments for determination of BET surface area, pore volume and pore size distribution. The flexibility in the number of analysis ports, there are 1-, 2-, 3-, 4- and 6-port instruments available, and many instrument options show how QUANTACHROME reacts to customer needs. This PARTICLE WORLD 5 presents the review article Determination of Specific Surfaces of Different Dimensions. This article can answer some questions of new instrument users, interested parties in the gas adsorption method and new customers of our LabSPA (Laboratory for Scientific Particle Analysis) for contract analyses and method developments in the field of porous solids, e.g. if one is interested to characterize specific samples as large pieces for example, samples with very small surface areas by use of krypton adsorption, microporous samples like zeolites, active carbons or MOF's or chemisorption to characterize catalysts. The new iSORB-HP completes the gas adsorption product line of QUANTACHROME for high pressure adsorption up to 200 bar!

Finally there are new developments also in the field of **characterization of powders:** The AQUADYNE DVS as one or two port dynamic gravimetric water vapour sorption analyzer is developed to characterize pharmaceuticals, foodstuffs, building materials and many others. Also the combination of particle size and shape analysis in the new sophisticated CILAS particle size analyzers are very welcome in the market as optimum in price performance.

Finally, and as support for you, we have created a complete list with actually 280 titles of our Application Notes on characterization of dispersions, powders and porous solids. You can load the actual list from **www.quantachrome.eu.com** under dates and downloads and can send your free of charge request to **info@quantachrome.de** to get the relevant articles as pdf.

Yours sincerely

Dr. Dietmar Klank

Articles in this issue:

Imprint

Editor:
QUANTACHROME
Office of Benelux
Schanspoort 21
NL-4791 HA Klundert
Phone: +31 168 370241
Fax: +31 168 405113
ton.goverde@quantachrome.nl
www.quantachrome.eu.com

Editorial Staff:
Dr. Dietmar Klank, Dr. Christian Oetzel, Matthias Lesti, Dr. Uwe Boetcher, Ton Goverde

Illustrations:
Quantachrome GmbH & Co. KG, Fotolia

Report of round robin test of zeta potential and particle size of dispersions with submicron sized particles

Dr. Uwe Boetcher
QUANTACHROME GmbH & Co. KG, uwe.boetcher@quantachrome.de

Dr. Gabriele Steinborn, Petra Kuchenbecker
(BAM) Bundesanstalt für Materialforschung und -prüfung, Fachbereich 5.5 „Technische Keramik“, Berlin

Sven Scheler
Universität Bayreuth, Lehrstuhl für Keramische Werkstoffe

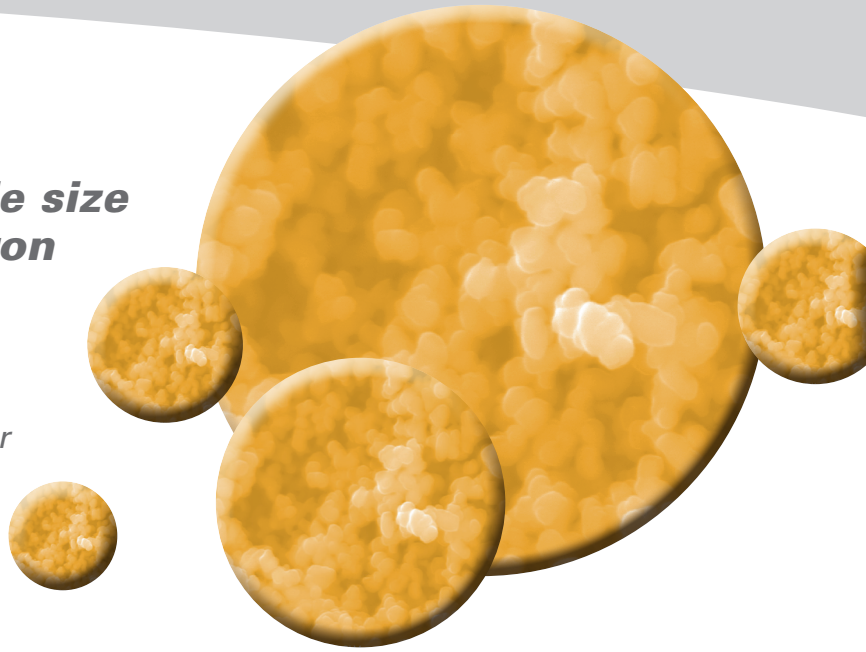

Scope

We report a round robin test from end of 2009, which was initiated and coordinated by the BAM (Bundesanstalt für Materialforschung und -prüfung, Berlin, Germany). The aim was to estimate the reliability of the acoustic and electroacoustic method which give access to particle size and zeta potential of concentrated dispersions. Ultrasonic spectrometers of Dispersion Technology were used at this round robin test.

Short introduction in the measurement technique

For more detailed information we refer to [1]. There are various methods to determine the zeta potential. One of them is electroacoustics, which enters an ultrasonic wave (3 MHz) into a concentrated dispersion. This wave leads to pressure variation which makes the particle oscillate. The oscillation shears away a part of the double layer, which results in generation of a dipole. The sum of these dipoles will be measured by two electrodes. The measured electroacoustic signal is then used to calculate the zeta potential.

The following procedure is used for determination of the particle size with acoustic attenuation: ultrasonic tone bursts are generated by a transducer within a range of 3 to 100 MHz and sent through a dispersion. A second transducer (linear arrangement according to the sound wave) will receive the damped acoustic wave. Usage of the coupled phase model of Dukhin and Goetz makes it possible to calculate the weight based particle size distribution from the attenuation curve. There is a norm for this procedure which was also used for these tests here. [2]

Benefits of measurement of zeta potential

Zeta potential is an important parameter to characterize and understand the charges of the particle surface and the repel forces of the particles. The bigger that forces are, the less effects like flocculation or aggregation will happen, which are synonymous for unstable dispersions.

The area of instability is important for materials like flocculants or for water treatment on the other hand. Deeper investigation of both areas, the stable and the instable one, are possible with variation of the pH through acid / base titration or addition of certain additives like flocculants and measurement of the zeta potential.

One should notice that the zeta potential is just of use for dispersions which are stabilised electrostatically, not sterical.

The round robin test

According to IUPAC rule a round robin test is…
„… a study, where different laboratories will measure a certain parameter of one or more identical portions of a homogenous and stable material under documented circumstances and will summarize the results in a joint report.“[5]

Therefore, various criteria have to be checked and prepared respectively prior to the performance of the round robin test itself.

E.g. a coordination is necessary which ensures the same age of the dispersion at the time of measurement in all laboratories to eliminate the influence of ageing of the dispersion. Calibration (electrical conductivity, pH-value and zeta potential) should be done in the same manner prior to the measurement additionally. Finally, the statistic report should be carried out by the initiator of the test according to (DIN ISO 5725-2). This norm e.g. clarifies how to treat outliers and near-outliers. [3, 4]. All listed aspects here were ensured by the BAM. Meaningful and reliable results could be achieved therefore.

Six (particle size) and seven (zeta potential) participants respectively took part for this round robin test.

Sample criteria and -preparation

Four different water based suspensions have been analysed according to table 1. Two of them have been suspensions and the other two of them powders, from which dispersions had been made of.

Table 1 *Specifications of the suspensions*

Sample No.	Dispersion	Manufacturer	Density/ g cm^{-3}	Average particle size/nm	Spec. Surface/ m^2 g^{-1}	Crystalline Phase
1	10wt% Al_2O_3-TM-DAR	Taimei Chemicals	3.99	~ 150	14.00	α-Al_2O_3
2	10wt% Al_2O_3-A16	Alcoa	3.99	~ 400	9.68	α-Al_2O_3
3	40wt%SiO_2 „Koestrosol“	CWK Bad Koestritz	2.20	< 100	185.00	amorphous
4	30wt%SiO_2 „Levasil 200“	Akzo Nobel	2.20	< 100	200.00	amorphous

The silica samples 3 and 4 have been measured without further treatment. The BAM tested optimum dose of dispersant Dolapix CE 64 (derivative of citric acid) prior to preparation of samples 1 and 2. Optimum dose was 1 % for sample TM-DAR and 0.6 % for Al_2O_3-A16 in relation to solid content. Amounts of 5 L of alumina suspensions had been prepared using following steps:

- Wet dispersion of powder in 0.001 molar KCl-electrolyte
- Addition of Dolapix CE 64
- 20 minutes ultrasonic treatment (Branson, Type „Sonifier 450“, 50 % pulsed)
- Stirring
- Sampling with 100 ml volumetric pipette

The samples were shipped to the labs at the day of preparation and measured there the next day.

Results

After receipt of samples 1 and 2 they were stirred for ten minutes at constant speed and put into the measurement chamber of the DT-1201 ultrasonic spectrometer and then measured there under stirring. Samples 3 and 4 were not stirred prior to measurement.

SEM-pictures including scaling of all 4 samples can be seen in figure 1 and 2. TM-DAR is a powder of corundum with nearly spherical particles. A16 is corundum as well, but shows irregular shape. The sols, shown in figure 2 are agglomerated after freeze-drying of the suspension. Both of them have got spherical primary particles, which are nano-scaled.

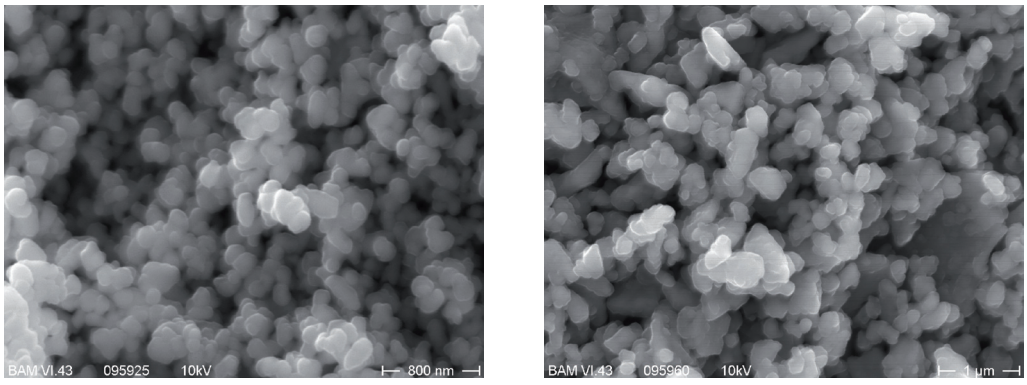

Figure 1
SEM-pictures of Al_2O_3-TM-DAR (left) and A16-Alumina (right); pictures made by Birgit Strauß.

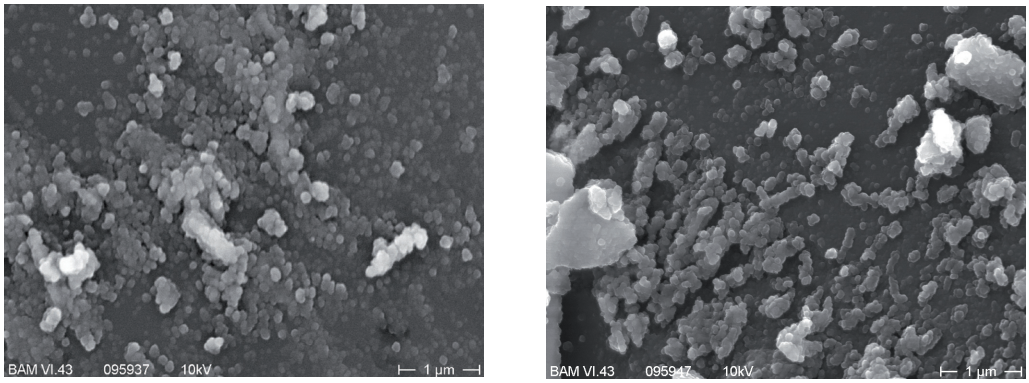

Figure 2
SEM-pictures of Koestrosol (left) and Levasil (right); pictures made by Birgit Strauß.

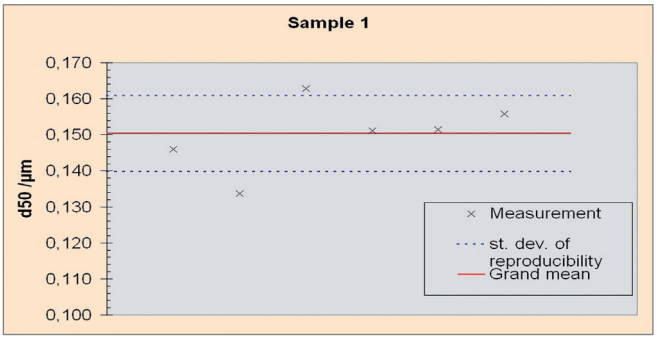

Figure 3 *Results of the 6 labs for average particle size d_{50} of sample 1*

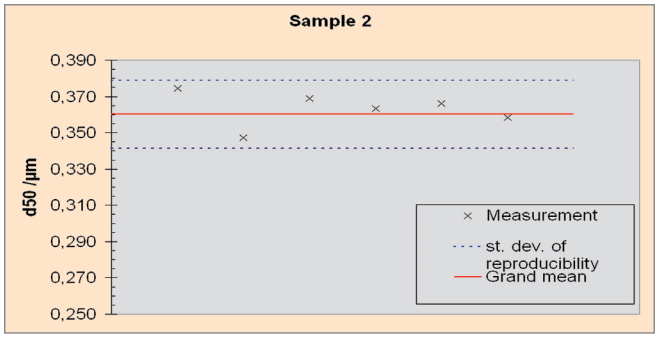

Figure 4 *Results of the 6 labs for average particle size d_{50} of sample 2*

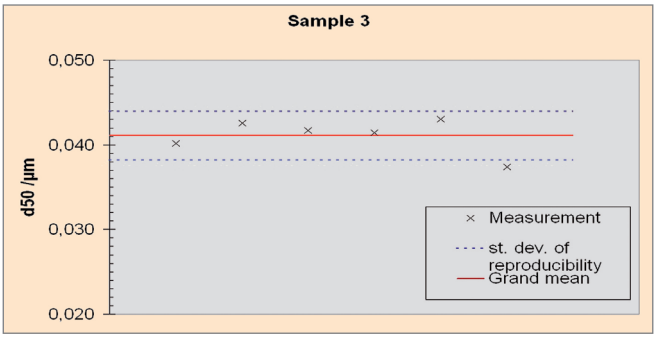

Figure 5 *Results of the 6 labs for average particle size d_{50} of sample 3*

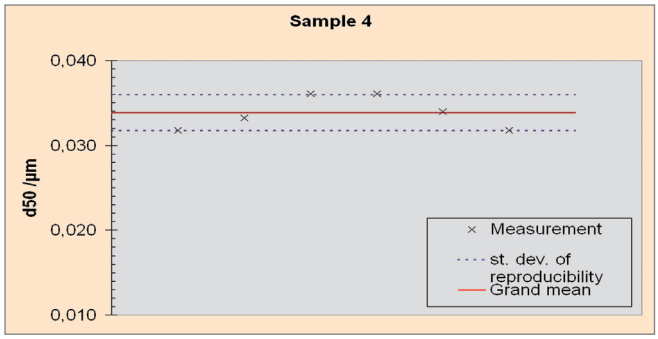

Figure 6 *Results of the 6 labs for average particle size d_{50} of sample 4*

Results and discussion of the particle size distributions

The results of the average particle size median d_{50} of the samples 1-4 are shown in figures 3-6.

Tables 2 and 3 list the results of the particle size distributions. The listed "repeatability standard deviation" is a value for the repeatability of the measurements in a given lab. The term "reproducibility standard deviation" is an estimated value of the variation of the procedure in general. For clarification of statistical values and terminology we refer to [5].

When looking at the d_{50}-values, it can be seen that the reproducibility standard deviation is never more than 7 %. So the labs are in good agreement here.

Results and discussion – zeta potential

Table 4 shows the results of the zeta potential measurement. Figures 7-10 show the averaged zeta potential. Two outliers were identified with Grubbs-test. They are marked in figure 9 and 10 and are therefore not involved in the data in table 4.

Table 2 *Overview of the particle size distributions and precision values of the Al_2O_3-samples*

	Sample 1-TM-DAR			Sample 2-A16-Al_2O_3		
	d_{10}	d_{50}	d_{90}	d_{10}	d_{50}	d_{90}
mean value /nm	64	150	353	121	360	1082
Repeatability standard deviation s_r /nm	4	4	16	7	15	109
rel. s_r /%	6.71	2.69	4.58	6.11	4.13	10.05
Reproducibility standard deviation s_R /nm	8	11	27	13	19	121
rel. s_R /%	12.17	7.02	7.76	11.11	5.22	11.22

Table 3 *Overview of the particle size distributions and precision values of the silica sols*

	Sample 3-Koestrosol			Sample 4-Levasil		
	d_{10}	d_{50}	d_{90}	d_{10}	d_{50}	d_{90}
mean value /nm	29	41	59	25	34	47
Repeatability standard deviation s_r /nm	3	2	2	2	1	3
rel. s_r /%	9.99	5.40	3.88	8.26	2.44	5.59
Reproducibility standard deviation s_R /nm	4	3	5	3	2	4
rel. s_R /%	12.78	7.02	7.66	12.42	6.26	7.82

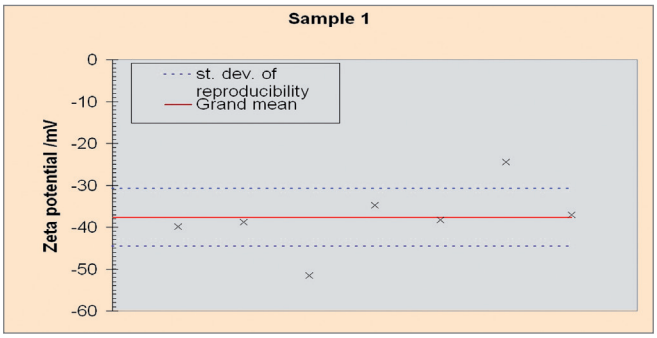

Figure 7 *average zeta potentials from each lab of sample 1*

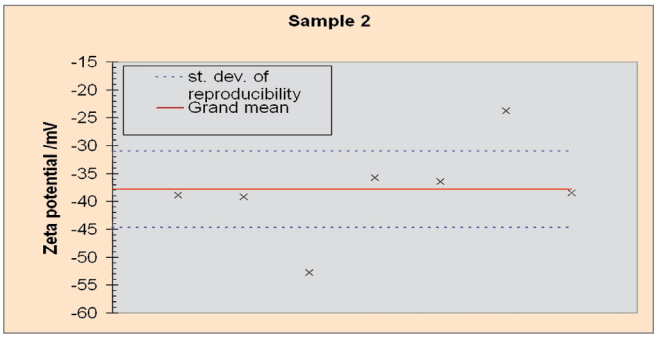

Figure 8 *average zeta potentials from each lab of sample 2*

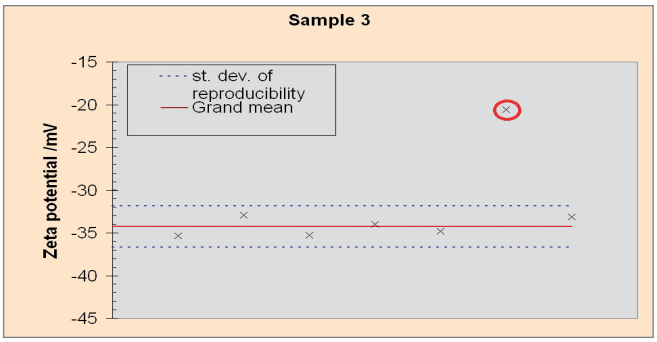

Figure 9 *average zeta potentials from each lab of sample 3*

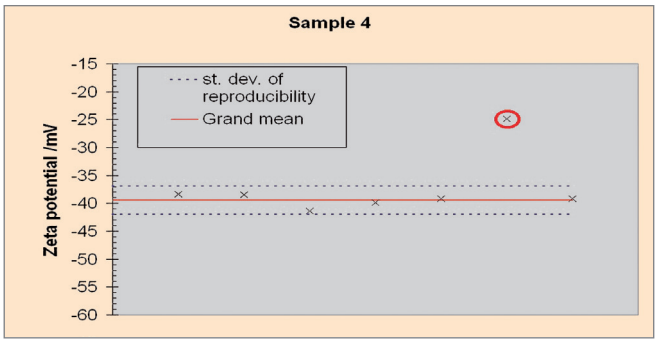

Figure 10 *average zeta potentials from each lab of sample 4*

Table 4 *Overview of the averages and precision values of zeta potential of the 4 samples*

	Sample 1 Zeta potential	Sample 2 Zeta potential	Sample 3 Zeta potential	Sample 4 Zeta potential
mean value /mV	-37.80	-37.90	-34.30	-39.50
Repeatability standard deviation s_r /mV	1.00	0.80	0.20	0.30
rel. s_r /%	2.68	2.14	0.61	0.70
Reproducibility standard deviation s_R /mV	6.90	6.90	2.40	2.60
Rel. s_R /%	18.27	18.12	7.05	6.50

Like for the particle size distribution, samples 3 and 4 show a good reproducibility standard deviation of around 7 %.

On the other hand, samples 1 and 2 show remarkable reproducibility standard deviations: figures 7 and 8 show that one lab measured a rather low average zeta potential, another lab measured a rather high one (within the six-fold measurement of zeta potential of each of the mentioned labs there was just low variation)

Additionally, the outliers of sample 3 and 4 have been measured by the same lab, which reported high values of samples 1 and 2. So, the reason could be some problem with the measuring unit.

Summary

As the measured samples are no reference materials, the results can not be checked regarding their correctness. But the results of the reported d_{50}-particle sizes of the different labs show good agreement. The commercial sols show also a good agreement in the geographical different places of the measurements.

Following institutes and companies took part in the round robin test: Universität Bayreuth, TU Braunschweig (IPAT), TU Dresden, Leibniz-Institut für Polymerforschung Dresden e.V., Quantachrome GmbH & Co. KG, Georg-Simon-Ohm Hochschule Nürnberg, Fachbereich Werkstofftechnik and BAM. We thank Birgit Strauß here, BAM, FB 6.8, for taking the SEM-pictures.

Literature

[1] *PARTICLE WORLD 3, QUANTACHROME GmbH & Co. KG, May 2009*

[2] *ISO 20998-1, „Measurement and characterization of particles by acoustic methods – Part 1: Concepts and procedures in ultrasonic attenuation spectroscopy", Genf 2006*

[3] *DIN ISO 5725-2, „Genauigkeit (Richtigkeit und Präzision) von Messverfahren und Messergebnissen - Teil 2: Grundlegende Methode für Ermittlung der Wiederhol- und Vergleichpräzision eines vereinheitlichten Messverfahrens" (ISO 5725-2:1994 einschließlich Technisches Korrigendum 1:2002), Beuth Verlag*

[4] *Frank E. Grubbs, "Sample Criteria for Testing Outlying Observations", The Annals of Mathematical Statistics. 21, Nr. 1, 1950, S. 27–58*

[5] *Danzer, K. et al. "Chemometrik – Grundlagen und Anwendungen", Springer Verlag, Berlin, Heidelberg, New York 2001*

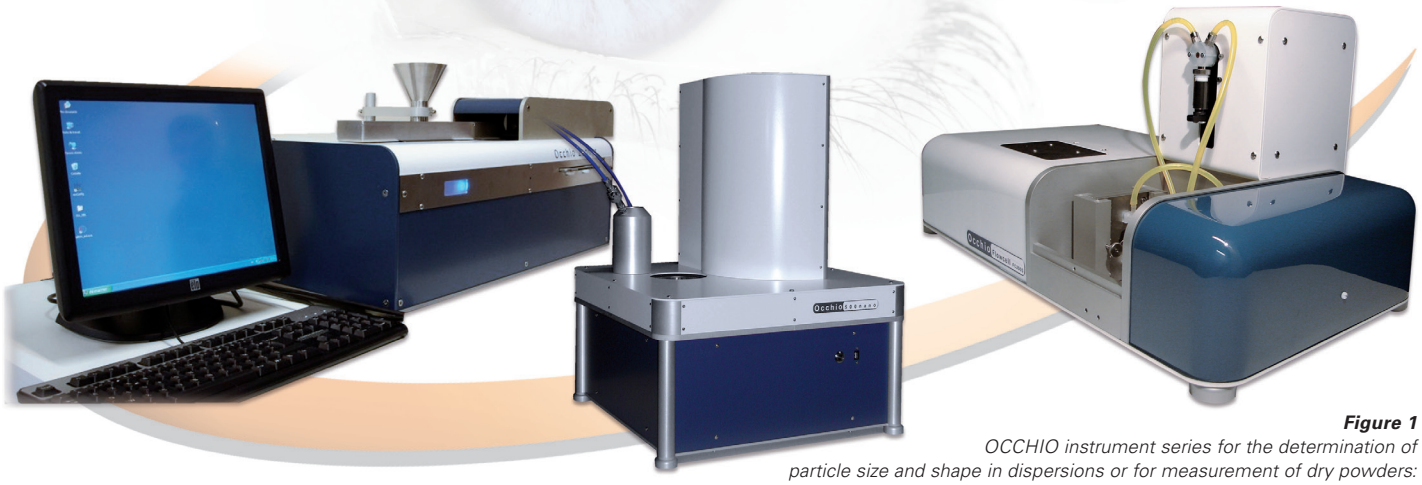

Figure 1
OCCHIO instrument series for the determination of particle size and shape in dispersions or for measurement of dry powders: ZEPHYR ESR (dry, optional wet analysis, left) from 20 µm - 3 cm, 500nano (dry, mid) from 0.4 – 2000 µm, FC200S+ (wet, right) from 0.4 – 1000 µm

Automatic image analysis for the determination of particle size and shape parameter distributions from 0.2 µm up to 3 cm

The combination of particle size and particle shape analysis becomes increasingly important for many tasks. Thus QUANTACHROME offers complementary to the particle analysis by laser diffraction a whole analyzer series for automatic image analysis (Figure 1). The OCCHIO analyzers determine coarse grained objects which allows very comfortable the automatic measurement of granules or other bulk materials with diameters up to 3 cm (ZEPHYR ESR, Figure 1 left; exemplary samples in Figure 2), as well as fine grained materials in fluid dispersion resp. as dry powders. Analysis results of dry measurements with the ZEPHYR ESR and the OCCHIO 500nano (Figure 1, mid-picture) are discussed in this article.

Figure 2
Powders, granules and bulk solids as possible sample types for the particle characterization with the ZEPHYR ESR (from left to right, top down): shredded plastics, fine crushed rock, sugar, various pellets, plastic granules, spicery, resp. sliced plant parts)

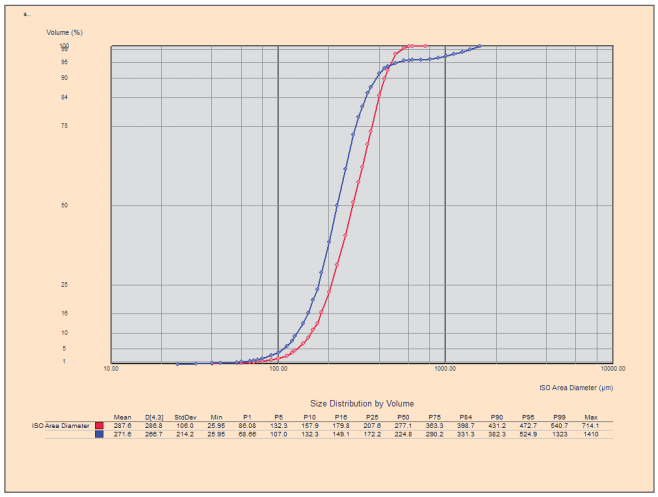

Figure 3 *Particle size distribution of a fine sand sample (red) in comparision with a building sand (blue), measured with the ZEPHYR ESR*

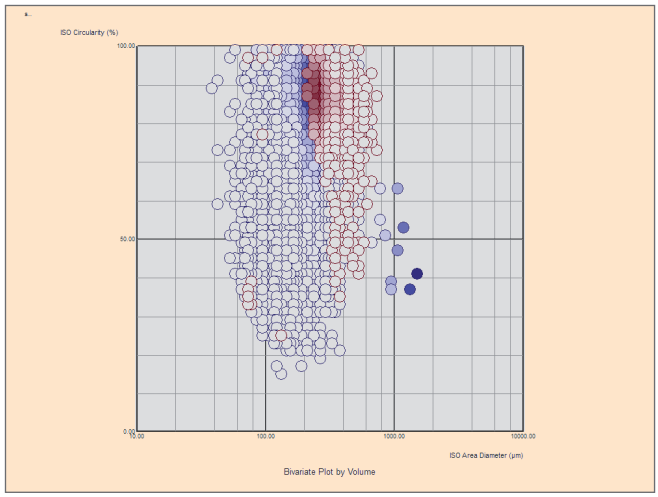

Figure 4 *Circularity of the two sand samples from fig. 3, represented vs. the area equivalent particle diameter, calculation with callisto-software of the ZEPHYR ESR*

The following analysis results illustrate the possibilities of the automatic image analysis regarding the characterization of rather coarse grained particles. The particle size distributions of two sands are shown in Figure 3. Only particle sizes < 800 µm are found in the fine sand, while the building sand contains ca. 4 % particles between 800 µm and 1,5 mm. Figure 4 highlights these results with respect to the share of coarse particles. The single blue dots on the right side are to be allocated to the bulk material of the building sand. The circularity of particles is plotted on the y-axis, the particle size on the x-axis (area equivalent diameter). The graph shows that the share of coarse particles of the building sand is of rather low circularity and thus deviates significantly from a circular particle shape. The Callisto software allows the imaging of every single particle and therefore a more exact particle shape determination of certain particles apart from the analysis evaluations shown here.

Figures 5 a, b and c show examplary at the determination of a coal sample how the results can depend on the chosen analysis parameters. It is the specific advantage of the automatic particle shape analysis against the faster laser diffraction analysis that not only a distribution of the sphere equivalent diameters gets calculated but that various particle dimensions can be analyzed and evaluated. Analyzed were different sizes of a coal sample with the ZEPHYR ESR. A shift of particle sizes towards the coarse area is noticeable between figure 5 a (top) and figure 5c (bottom), which is caused only by different ways of evaluation. The volume

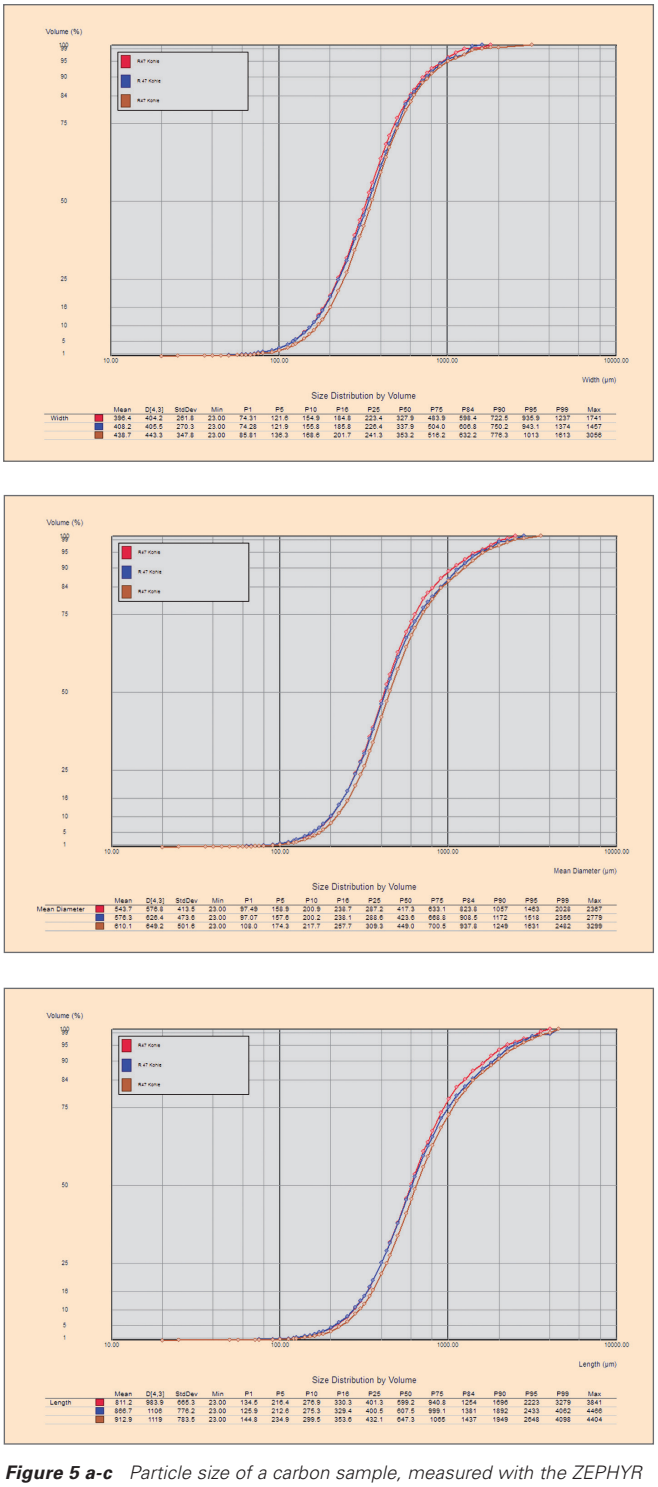

Figure 5 a-c *Particle size of a carbon sample, measured with the ZEPHYR ESR, represented vs. particle width (5a, top), vs. median particle diameter (5b, mid) and vs. particle length (5c, down)*

distribution was plotted above the particle width in Figure 5a (top), the D50-value is about 340 µm, the D90-value at about 750 µm. Figure 5 (in the middle) shows the volume distribution against the average particle size diameter, the D50-value shifts towards ca. 430 µm, the D90-value towards 1200 µm. In Figure 5 (bottom) the D50-value is at ca. 620 µm and the D90-value at 1600 µm, as the particle length distribution is depicted here. The stronger the distributions of the three chosen linear dimensions differ, the stronger the particle shape deviates from the sphere form and rather equates e.g. elliptical- or rod-shaped particle shapes.

The wide measurement range of the ZEPHYR ESR is clearly visible in Figure 6, in which the particle size distributions of the multiple measurements of coffee beans (right), coffee powder (mid-picture) and fine sugar (left) are shown. (Note for 'scientific milk-coffee drinkers': QUANTACHROME provides also for the determination of the size of fat droplets in milk and the milk´s durability (stability of dispersions) appropriate analysis technique!)

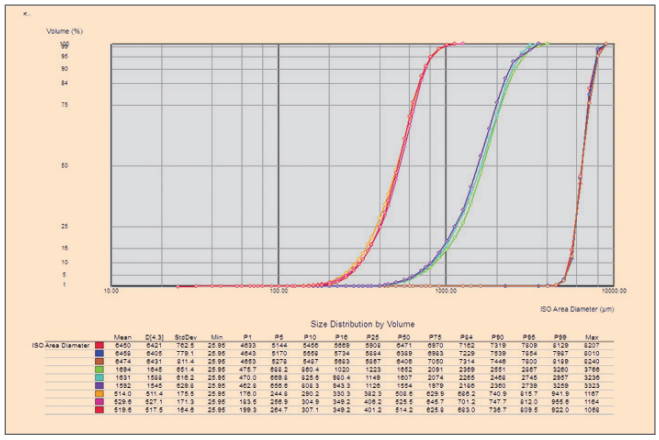

Figure 6 *Particle size distribution (area equivalent) of coffee beans, coffee powder and fine sugar, analyzed with the ZEPHYR ESR*

The possibility to display special length dimensions at the characterization of fibres is especially interesting, as the given tasks can vary strongly and other analysis methods often don´t bring the required results. Three samples of cellulose fibres with a thickness of ca. 15 µm were examined as an example. Figure 7a depicts clearly the overlapping of the size distributions in regard to the thickness of the fibre, the differences in fibre thickness between the samples are not significant. Figure 7b otherwise shows the volume distribution throughout the max. object length and substantial differences are to make out as 1 % of the fibre lengths of the three samples is smaller than 70 µm, 56 µm resp. 29 µm and the D50-value shifts from 412 µm to 349 µm to 320 µm. Different fibre characteristics can therefore be evaluated with the image analysis, which are either not at all detectable with other analysis methods or at least don´t bring absolute values, which in the case of the example was the size distribution of the fibre length. The image analysis used for fibre characterization has the additional advantage that the fibres don´t have to be stretched to determine the fibre length but can be curved or curled, as ever the largest or, for the determination of the fibre thickness the smallest fibre dimension out of the max. contiguous amount of pixels of the particle image is calculated.

The illustrated results show numerous analysis possibilities of the automatic image analysis at the measurement of dry powders and granules. However for the sake of completeness it should be noted that especially very fine powders ought to be dispersed (a dispersion option is implemented in the OCCHIO 500nano). Besides QUANTACHROME offers dry dispersion and – measurement within the scope of the traditional laser diffraction for particle size analysis.

Analyzers with dry as well as liquid dispersion are provided in our LabSPA (Laboratory for Scientific Particle Analysis) for you. Graphs show the measurement ranges of our particle size analyzers at the back side of this Particle World but according information is also available at our homepage **www.quantachrome.de**.

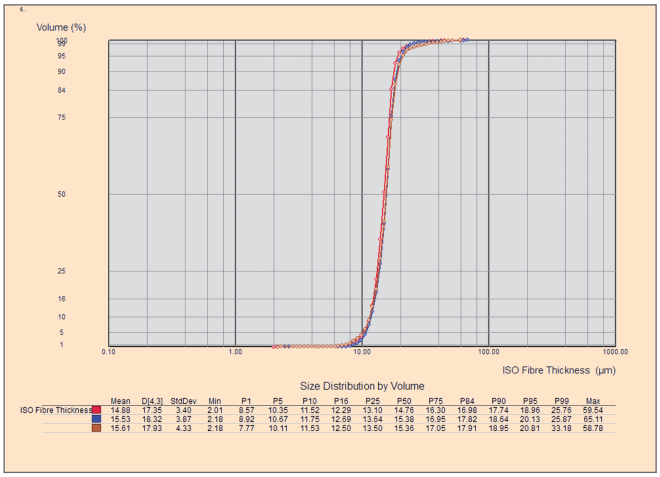

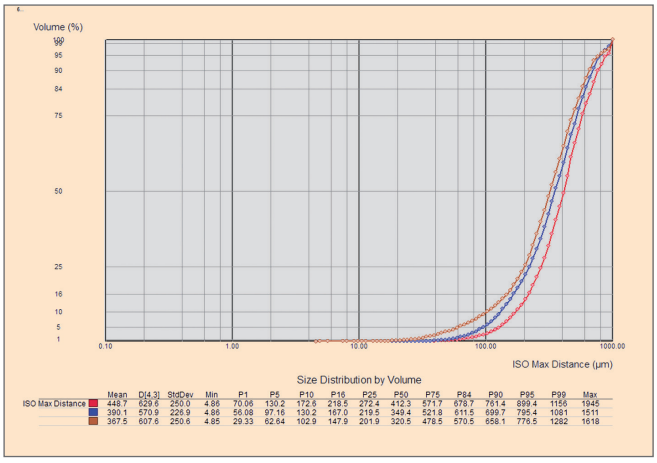

Figure 7a-b *Size distribution of cellulose fibres: While the fibre widths (7a) are not distinguishable, the differences in fibre lengths are significant (7b), analyzed with the OCCHIO 500nano, calculated with the software Callisto*

POROMETER series for characterization of filters, membranes, papers, textiles and other materials with through-pores

Figure 1
POROMETER 3G zh to characterize through-pores in the range 0,018 to 500 µm

Figure 2
Porofil: the liquid with very low surface tension (just 16 mN/m), will even wet polytetrafluoroethylene (PTFE), is chemically inert, will not swell materials like water and alcohol can and can be used with all types of porometers

The POROMETER 3G series is a compact, automatic, wide size range, low flow and high flow rate capable capillary flow POROMETER for measuring through-pore sizes using the liquid expulsion technique, plus gas (and optionally liquid) permeability. Gas pressure is applied to one side of a wetted sample and the resulting flow rate, through pores that empty as the gas pressure increases, is measured. The principal pressure capability of the technique allows for pore size distributions in the range of 0.018 to 500 µm to be measured quickly and reproducibly on a wide variety of materials like woven and non-woven filter materials, membranes, papers, sintered metals, etc. according to ASTM standard methods D6767, E128, F316, and similar.

Pore Size Methodology

All 3G POROMETERS (Figure 1) employ the same technique of expelling a wetting liquid from through-pores in the sample. Gas pressure is automatically applied to one side of the sample and as pores empty the resulting gas flow through the open pores is accurately measured by the on-board microprocessor. The actual pressure at the sample is measured independently of the pressure control circuit to ensure the highest quality data. The preferred wetting liquid, Porofil, has been selected because of its special physical properties (Figure 2). An optional External Sample Manifold facilitates work with non sheet-like materials such as hollow fibers and cartridges.

Permeability Methodology

All 3G POROMETERS can also measure permeability. Without modification they can acquire gas permeability data at a single desired pressure, with stabilization defined by pressure or flow, and across a range of pressures at chosen stabilization times. Liquid permeabilities can also be determined using an optional accessory (Figure 3).

Figure 3 *Option for the determination of the liquid permeability by use of the POROMETER 3G instrument series*

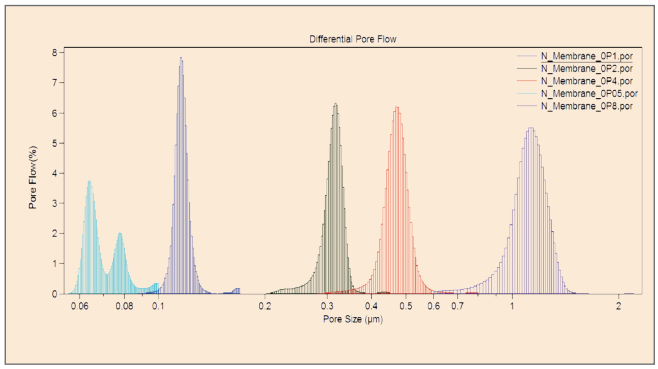

Figure 4 *Through-pore size distributions of five different membranes, measured with the POROMETER 3G zh.*

Pore Size Range

The pore size measuring capability of a porometer is dependent on its pressure range capability. The 3G series offers a sufficiently wide pressure range to be able to analyze from less than 20 nm to about 0.5 mm. The 3G zh has the widest pore size range from < 0.02 microns up to 500 microns. The 3G z can measure much of the same range as the 3G zh, but for the smallest pores. The 3G macro is recommended for applications involving only larger pores, from 0.09 to more than 500 microns with enhanced resolution. The 3G micro specializes in measuring over narrow pore size ranges within an overall range of 60 to 90,000 nm. Figure 4 shows the pore size distributions of five different membranes, measured with the POROMETER 3G zh.

Pressure Control and Measurement

Optimal performance for very different pore size applications requires different pressure ranges, hence the four models of the POROMETER 3G series. All 3G models but for the 3G micro are equipped with two controllers covering the appropriate pressure ranges. The 3G zh has no less than three pressure sensors, 0-5 psi, 0-100 psi and 0-500 psi. The 3G has a similar configuration, but is limited to 250 psi. The standard 3G micro and 3G macro have the same low and medium pressure sensing range as the z and zh, i.e 0-5 psi, and 0-100 psi, but the 3G micro is also offered with an alternative medium pressure range of 0-150 psi.

Flow Rate

Pressure is just one aspect of porometry. The other is flow rate. As the pressure is increased to empty smaller and smaller pores of the wetting fluid, gas flow continues through previously opened pores, and must be continuously and accurately measured. A small number of pores results in a low flow, a larger number of pores results in a larger flow. The same number of large pores as small pores also results in a higher flow rate. The wide range 3G zh therefore has two flow sensors (0-10 and 0-200 L/min) with automatic switching between the two. The standard 3G z is offered with one flow sensor (100 L/min) but can be optionally fitted with a second sensor (5, 50 or 200 L/min) to encompass more applications. The 3G macro, specializing in large pore applications, therefore features a high-flow rate sensor (0-200 L/min), while the 3G micro is offered with a 0-100 L/min sensor as standard, or one may choose to substitute a lower flow (0-20 L/min) or a higher flow (0-200 L/min) sensor for specific (e.g. quality control) applications.

Figure 5 *Open sample holder of the POROMETER 3G for flat filter samples*

Sample Holders

Different applications don't just mean different pore sizes (pressures) and flow rates, but also different sample sizes. Samples come in different diameters and thicknesses. And so to comfortably accommodate your samples, all 3G POROMETERS come with an exchangeable sample holder (Figure 5): most popular is the 25 mm diameter and is available as standard on all models. Other single diameter holders available are 18 mm, 37 mm and 47 mm, or you may prefer the universal 10-50 mm holder if you work with very many different sample types. Loading and unloading samples is facilitated by the sample holder being freely accessible.

If you are interested in more information about the characterization of through-pores in filters, membranes or similar materials, do not hesitate to send your request to **info@quantachrome.de**.

Application notes and other literature on characterization of dispersions, powders and porous solids

You can find plenty of information and papers on our websites **www.quantachrome.eu.com** (resp. **www.quantachrome.nl** or **www.quantachrome.dk**) and at the hompepages of

- FORMULACTION (France) at **www.formulaction.com**
- DISPERSION TECHNOLOGY (USA) at **www.dispersion.com**
- CILAS (FRANCE) at **www.cilas.com/particle-size-analyzer.htm**
- OCCHIO (Belgium) at **www.occhio.be**
- QUANTACHROME Instruments (USA) at **www.quantachrome.com.**

To offer a help to find the application note related to your favorite topics, we prepared a new list of application notes with numbers and key words in Excel-format for easy search and easy send of your request to us.

An example is shown for the characterization of dispersion in the way of stability measurement of dispersions, phase behaviour, rheological measurements with DWS and film formation (drying / curing) investigations. The table is sorted here for different branches of industry. The numbers are related to the numbers of Application Notes from the complete list which you can download from our hompage:

www.quantachrome.eu.com
under > **Dates and Downloads**
> **Application Notes**

If you are interested in one or more entries below, please mark interests in the left column and send us the copy as fax (+49 (0) 8134 93 24 25) or as scanned file by email to **info@quantachrome.de**. You should enter your email address too, only in this way we can send you the required application notes, free of charge of course. Another way, and with access to all about 300 application notes, is to load the xls-file from **www.quantachrome.eu.com** and to send it filled to **info@quantachrome.de**.

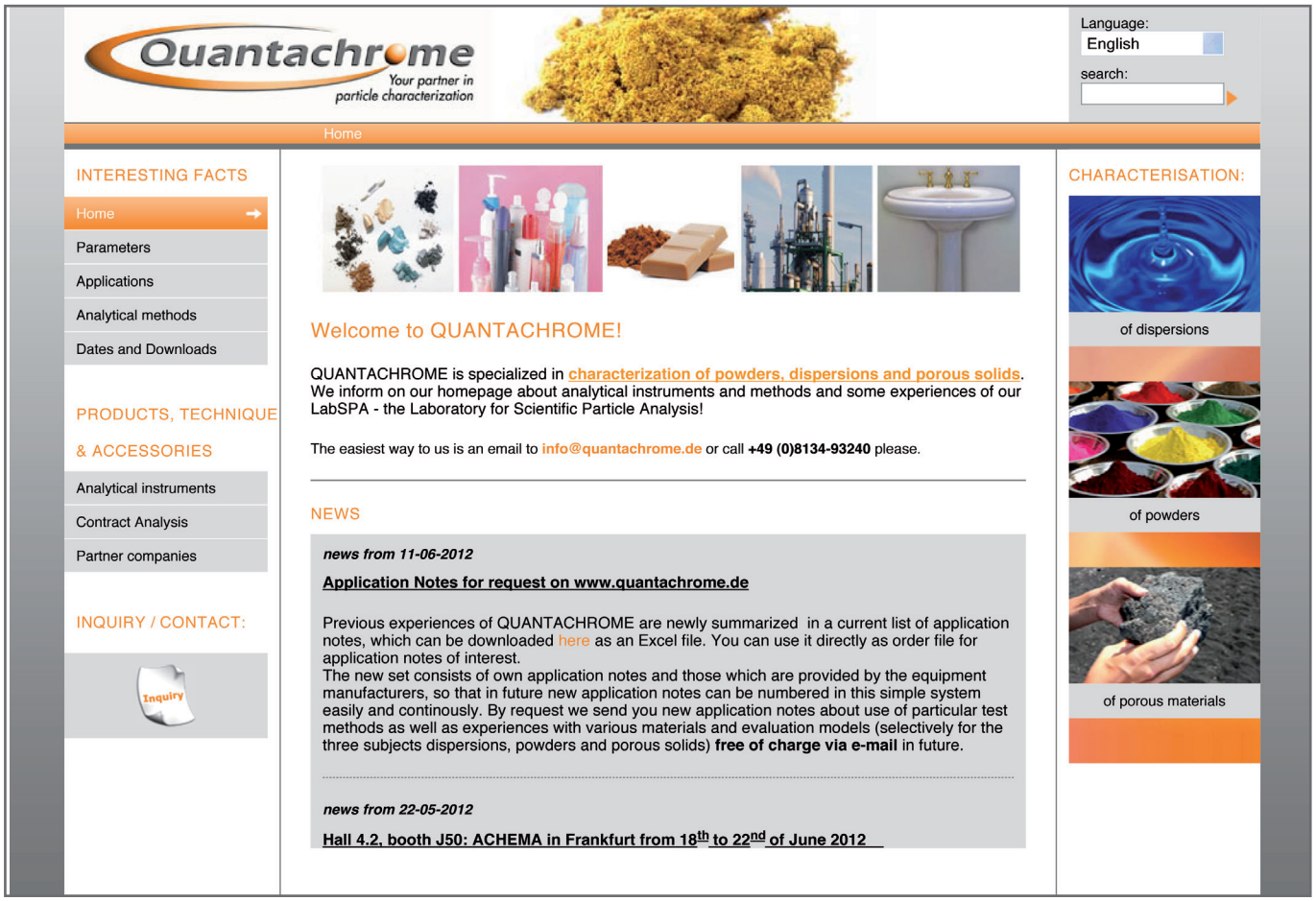

Paints and inks

	Number*	
❐	54	Stability of pigment inkjet inks
❐	55	Effect of the introduction of polymer on pigment dispersion stability
❐	56	Study of the stability of a ceramic ink
❐	57	Stability and use properties of pigment based inks
❐	58	Optically measuring drying of black or blue inks
❐	59	Curing of a UV-ink
❐	60	Choosing the right coalescent
❐	61	Switching to an environmentally friendly drier
❐	62	Finding the right open time
❐	63	Changing pigment
❐	64	Drying mechanism of water-based coatings

Cosmetics

	Number*	
❐	77	Effect of raw materials on a formulation
❐	78	The effect of ingredient quality on final formulation stability
❐	79	Characterization of an emulsion
❐	80	Identification of the instability phenomenon of an emulsion
❐	81	Formulation of direct emulsions
❐	82	Study of the quick breaking of a foam
❐	83	Study of the slow breaking of a foam
❐	84	Pre-formulation of a double emulsion
❐	85	Study of the release of an encapsulated active in a double emulsion
❐	86	Study of the gelling of an emulsion
❐	87	Development and control of cosmetics products
❐	88	Behaviour of a 'no transfer' face foundation
❐	89	Thixotropy of gloss lipstick
❐	90	Behaviour of a 'no-clump' mascara
❐	91	Effect of a process on the viscoelastic properties of a body cream
❐	92	Rheological analysis of toothpastes
❐	184	Stability of cosmetic emulsions
❐	185	Stability of pickering emulsions
❐	186	On line monitoring of emulsions for scale-up
❐	187	Multiple emulsions

Food

	Number*	
❐	65	Stability of various beverage emulsions
❐	66	Effect of fat content on the creaming of milk
❐	67	Effect of the temperature on the clarification of the wort in the beer making process
❐	68	Study of yoghurt formation
❐	69	Formulation of a chocolate milk
❐	70	Stability of whipped egg
❐	71	Study of the making of sponge cake
❐	72	Development and control of beverage emulsions
❐	73	Viscoelastic characterization of cheese thanks to microrheology
❐	74	Study of yogurt textural properties
❐	75	Optimizing the texture of a low-fat emulsion
❐	76	Optimizing the cost of a low-fat emulsion
❐	162	Mesostructure of fibrillar bovine serum albumin gels
❐	163	On Line bubble size measurement using a multiple light scattering sensor
❐	164	Phase stability of concentrated dairy products
❐	165	Lactoglobulin effect on depletion floc
❐	166	Measurement of layer formation in dairy emulsion
❐	167	Phase separation on aqueous starch systems
❐	168	Particle size and stability of milks
❐	169	Weighting agent
❐	170	Sodium caseinate emulsion and foam
❐	171	Foam stability
❐	172	Emulsion flocculation
❐	173	On line monitoring of foam
❐	174	Phase separation of starch/xanthan mixtures
❐	175	Recombined dairy cream
❐	176	Microencapsulated sunflower seed oil
❐	177	Filtration of food salting solutions
❐	178	Stability of food foam
❐	179	Complexation in solution
❐	180	Xanthan and Weighting agents
❐	181	Stability of acidified milk drinks
❐	182	Modified egg yolk emulsifying properties
❐	183	Emulsion crystallisation

** Number in the list of application notes according the xls-file from www.quantachrome.eu.com*

Pharmaceuticals

	Number*	
❐	93	Loading and delivery of a pharmaceutical drug in an hydrogel
❐	94	Development of pharmaceutical products
❐	95	Stability of pharmaceutical products
❐	96	Effect of an antibiotic on the stability of injectable emulsions
❐	97	Effect of electrolyte introduction on injectable emulsion stability
❐	188	Effect of dilution on drug dispersion
❐	189	Study of emulsion stabilization using polymers
❐	190	Formulation of submicronic emulsions by using high pressure homogenizer
❐	191	Kinetic formation of drug
❐	192	Sedimentation characterization of ophthalmic suspensions
❐	193	Surfactant particle interaction
❐	194	Stability of inhaler suspensions
❐	195	Characterization for formulation design
❐	196	Insuline W/O/W emulsion
❐	197	Parenteral emulsion stability
❐	198	Polysaccharide nanoparticles
❐	199	Nanogels
❐	200	Stability of emulsions for parenteral feeding
❐	201	pH sensitive MWCNT for drug delivery
❐	202	Nanosphere for ocular treatment

Surfactant

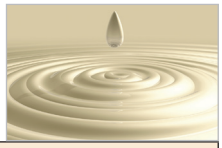

	Number*	
❐	98	Control of the quality and performance of surfactants
❐	99	Detergency properties of surfactants
❐	100	Foamability of a surfactant
❐	101	Stability of foams

Agrochemical

	Number*	
❐	109	Effect of the water hardness
❐	110	Formulation of a concentrated emulsion for natural agrochemical

** Number in the list of application notes according the xls-file from www.quantachrome.eu.com*

Electronic

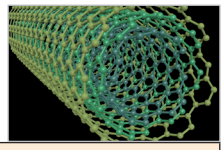

	Number*	
❐	102	Stability of suspensions for electronic applications
❐	103	CMP slurry stability
❐	104	Stability of platinium nanoparticles in fuel cells
❐	105	Dispersability of multi-walled carbon nanotubes
❐	203	CMP slurries
❐	204	Nano pigment screen display
❐	205	Transparent film of carbon nanotubes
❐	206	Stability of multi-walled carbon nanotubes
❐	207	Stability of nanofiber aqueous colloids
❐	208	Silver nanoparticules
❐	209	Stability of pristine carbon nanotubes
❐	210	Encapsulation of multi-walled carbon nanotubes
❐	211	Phosphor inks for ink-jet process in PDP
❐	212	Stability of carbon black dispersion

Oil and petroleum

	Number*	
❐	106	Quality control of self-emulsifying oils and lubricant emulsions
❐	107	Stability of petroleum oil
❐	108	Stability analysis of drilling fluids thanks to microrheology
❐	213	Development of new green demulsifiers for oil production
❐	214	Role of polyelectrolyte dispersant in the settling behavior of suspensions
❐	215	Formulation of a bitumen emulsion
❐	216	Novel method to study oil stability
❐	217	Lubricant emulsion stability
❐	218	Mechanism of crude oil demulsification
❐	219	Lubricating emulsions
❐	220	Stability of diesel-bioethanol fuels
❐	221	Drilling fluid
❐	222	Stabilisation of asphaltenes
❐	223	Metalworking fluids
❐	224	Asphaltene adsoprtion on minerals
❐	225	Demulsification of crude oil emulsions: a review
❐	226	Stability of suspensions
❐	227	Electrical field demulsification

Polymers

	Number*	
❐	111	Kinetics characterization of two gelation processes
❐	228	Stabilisation of emulsions by PVA
❐	229	Emulsifying properties of insoluble polymers
❐	230	Emulsions for elastometric films
❐	231	Flocculation with polymer flocculants
❐	232	Latex modification
❐	233	Polyurethane dispersion
❐	234	Polystyrene microsphere
❐	235	PVA suspension polymerisation
❐	236	Cross-linked micelles
❐	237	Stability of high internal phase emulsions

General

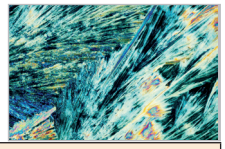

	Number*	
❐	112	Set up a stability method
❐	113	Soft matters end use properties analysis thanks to microrheology
❐	238	New technology for advanced drying analysis of coatings
❐	239	New technique for the analysis of microstructure dynamics, drying processes and coating formation
❐	240	Film formation of coatings studied by DWS
❐	241	Film formation analysis by optical method
❐	242	Optical film formation analysis
❐	243	Film formation analysis by diffusive wave spectroscopy

Slurries

	Number*	
❐	264	Ceramic foam
❐	265	Spray dried ceramics
❐	266	Nanofluid
❐	267	Nanopowders ceramic
❐	268	Polyurethane foams
❐	269	Ceramic nanoparticles from nanoemulsions
❐	270	Stability-flotation of silica
❐	271	Sedimentation behaviour
❐	272	Suspension settling
❐	273	Silica composite particles
❐	274	Sedimentation of bentonite
❐	275	Stability of concentrated suspension
❐	276	Stabilisation of mullite coating
❐	277	Stability parameter of mineral suspension
❐	278	Green bodies fabricated by tape casting

Different topics

	Number*	
❐	114	Effect of the positive Ion nature on the carbonate dissolution efficiency
❐	115	Effect of flocculating agent concentration on the flocculation efficiency
❐	116	Charge effect of flocculating agents on the flocculation efficiency
❐	117	Effect of the homogenisation speed on the emulsification efficiency
❐	118	Characterization of phase inversion
❐	119	Effect of the stirring power on the emulsification efficiency
❐	120	Sensitivity to size variation
❐	244	Creaming of flocculated emulsions
❐	245	Dependence of creaming on particle size and concentration
❐	246	Kinetics of droplets aggregation
❐	247	On line study of emulsification process
❐	248	Latex shear optical study
❐	249	Probing floc structure
❐	250	Identification of optimum formulations
❐	251	Depletion and bridging flocculation
❐	252	Dextran induced depletion flocculation
❐	253	W/O nanoemulsion
❐	254	Phase transition of emulsions
❐	255	PIT determination
❐	256	Online monitoring of coagulation for water treatment
❐	257	Phase separation for black liquors in wood cooking
❐	258	Low energy emulsification
❐	259	Bioflotation and bioflocculation
❐	260	Low energy nanoemulsion
❐	261	One-step preparation method of multiple emulsions
❐	262	Characterization of a two-aqueous phase system containing a nonionic surfactant
❐	263	Soil remediation
❐	279	On Line emulsification process monitoring and control
❐	280	Characterization of concentrated emulsions: application to formulation and quality control
❐	281	On Line characterization of particle size during grinding
❐	282	Particle size and rapid stability analyses of concentrated dispersions

** Number in the list of application notes according the xls-file from www.quantachrome.eu.com*

A contribution to the recently published definition for "nanomaterial" of the European Union (EU)

Dr. Uwe Boetcher, uwe.boetcher@quantachrome.de
Matthias Lesti, matthias.lesti@quantachrome.de

The subject "nanomaterial" has been discussed controversially for more than ten years. This discussion is fed with the new definition of "nanomaterial" given by the European Union. The most important question seems to be, if there is a risk for health based on an introduced nanoparticle containing material. Other questions in this context are safety or environmental issues.

Nanomaterials are very interesting for several reasons. The melting point of gold nanoparticles (~10 nm) for example is measured with 930°C more than 100°C lower than for other bigger gold particles [1, 2]. Semi-conducting materials like CdSe can be controlled regarding their optical and electronical properties via their particle size distributions. M. Faraday et. al. introduced the particle size dependence of an emission spectrum for gold suspensions in 1847.

This article shows the possibilities and problems of the analytical techniques to answer the following question: "Is this a nanoparticle by definition or not?"

First of all it is important to look at the original text published in October, 2011, by the European Union:

„The current definition is based on the consideration of the size of particles and not of the potential risks of them. A nanomaterial is described as *„a natural, incidental or manufactured material containing particles, in an unbound state or as an aggregate or as an agglomerate and where, for 50 % or more of the particles in the number size distribution, one or more external dimensions is in the size range 1 nm – 100 nm." [3]*

Regarding to analytical techniques, there is one important expression in this text: „number size distribution". There are several instruments available on the market which measure the volume or weight based particle size distribution of a material. Both distributions can be transformed in a number size distribution according to the transformation method of Hatch and Choate [4]. But this method is controversially discussed, too.

A number size distribution arises by definition with methods where the particles are counted. Alternatively, one can get number based distributions with microscopic methods.

The expression "in one or more external dimensions" shows, that the other important parameter is the particle shape. In consequence, there are only analytical methods allowed providing these two parameters: microscopic methods like SEM. One disadvantage of these methods is the difficulty of representative sampling. One can analyse only a very small

part of the sample, which is in the most cases not representative enough. Secondly, this method is very time consuming. That's the dilemma of measurement techniques: There are methods providing both parameters but they are too time consuming and too expensive.

The compromise should be a measurement technique, which

- shows the presence of a relevant number of nanoparticles or
- indicates the presence of nanoparticles

Laser diffraction is a well established method to determine sizes in the micrometer range. In the relevant range < 100 nm, this technique becomes insensitive. Nevertheless, if a dispersion is measured with a laser diffraction instrument, and all detectable particles are in nanometer range with the biggest fraction < 100 nm, then this would indicate a nanomaterial by the EU definition.

Methods

Laser diffraction

The granulometers of the CILAS series are working to the standard ISO-13320-1. During the analysis, a focused laser beam strikes on the particles to be analysed. The interactions between the laser beam and the particles lead to a characteristic light intensity distribution in direction of propagation. This pattern, which is characteristic for the sample, is used to calculate the particle size distribution.

According to the ISO standard, the software offers the analysis of the raw data according to two theories, which should be applied in dependence of the particle size range: the first is the Fraunhofer theory, which describes the appearance of the characteristic intensity distribution on the basis of Huygens principle and the geometrical optics using light diffraction (far field approximation). The second is the Mie theory, which will be particularly applied for particles smaller than the wave length of the light. The characteristic light intensity distribution can be described by scattering of the electromagnetic light wave on the particles. In this case, the knowledge of the complex refractive index is necessary in order to do the correct analysis [5].

Acoustic spectroscopy

The acoustic spectroscopy produces data, which are used to determine particle size distribution and rheological properties of concentrated dispersions. The DT-1202, DT-600 and DT-100 measure sound attenuation and velocity of any fluid-like material according to the "tone-burst-method". Sound pulses are transmitted through the sample. The attenuation of these pulses is measured over a wide range of ultrasonic frequencies (1-100 MHz) using variable gap sizes between ultrasonic transducer and receiver. The particle size will be calculated from the measured spectrum based on latest theories for attenuation of acoustic waves at colloidal particles. The wide range of ultrasonic frequencies enables the measurement of very small (<< 100 nm) as well as coarser particles (>> 5 µm). Because of the variable gap size the DT-spectrometers offer highest capability and flexibility regarding the range of concentration of the dispersion. Strong diluted (> 0.1 vol-%) and high concentrated systems (> 50 vol-%) can be characterized and no calibration is necessary. The software takes into account several mechanisms of ultrasound interaction with the colloid particles including scattering, viscous dissipation and thermodynamic coupling [6].

Experimental setup and results

This chapter describes experiments and results showing the possibilities and problems of a complete characterization of a nanomaterial regarding to its particle size.

Materials

The material to be analysed is a 10 % (wt.-based) aqueous silica dispersion. The disperse phase consists of two fractions in equal parts by mass of silica 1 and silica 2 (see table 1). Because of the fifty-fifty composition it is expected, that the mixture fulfills the term "nanomaterial" by definition, because the number of silica 1 particles is much higher than the one for silica 2.

Table 1 *Used materials and their key parameters*

	d_{50} / nm	density / g/cm³	refraction index / –
Silica 1	25	2.20	1.457 (at 635 nm) [7]
Silica 2	110	2.17	1.457 (at 635 nm) [7]

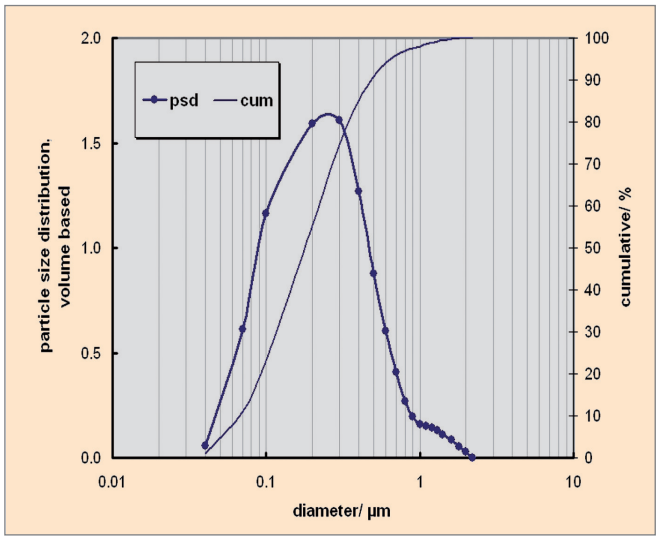

Figure 1 *Particle size distribution of the mixture of silica 1 and silica 2 (50/50) carried out with laser diffraction (volume based)*

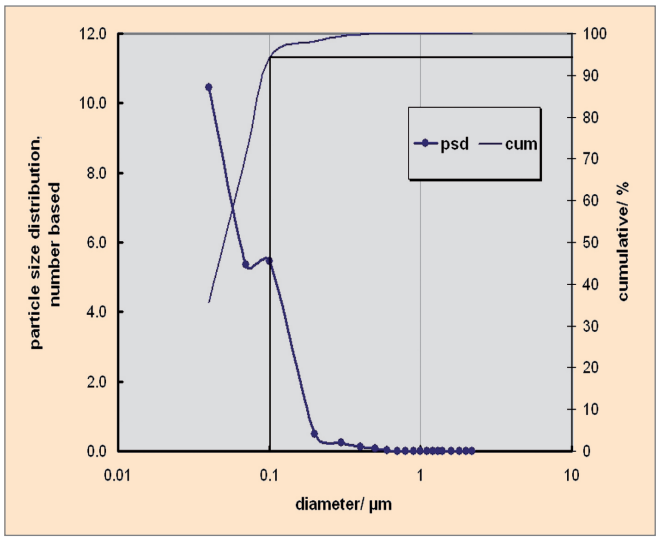

Figure 2 *Particle size distribution of the mixture of silica 1 and silica 2 (50/50) carried out with laser diffraction (number based)*

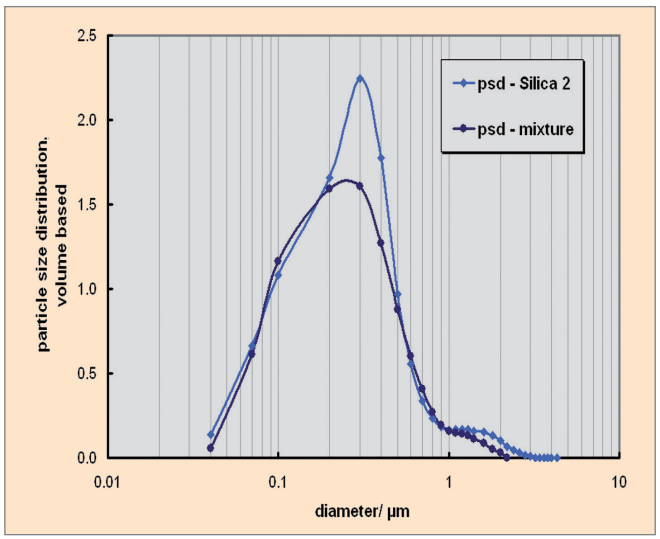

Figure 3 *Comparison of the particle size distribution of the mixture and silica 2*

Laser diffraction (static light scattering)

The laser diffraction measurements were carried out by a Cilas 1090L. The sample was sonicated during the experiment (30 Watt) in order to avoid agglomeration. Figure 1 shows the volume based particle size distribution, determined with Mie theory.

The volume based particle size distribution shows, that 23 % of all particles are detected smaller than 100 nm. This indicates, that the fine fraction (d50~25 nm) is not detectable with this method. The determined number based distribution (see figure 2) states the result: The analysed material is a nanomaterial. Based on counting method, laser diffraction detects more than 90 % smaller than 100 nm.

To get more information of the influence of the small particles on the laser diffraction method, the sample silica 2 was analysed separately. Figure 3 shows no significant difference especially in the range < 200 nm for both measurements. In consequence, we can conclude, that the material silica 1 is completely ignored by the laser diffraction instrument.

For the most cases, a laser diffraction instrument like CILAS 1090L is absolutely adequate to get the information if a material is nano or not by EU definition. On the other hand, to get trustable information on the real particle size distribution of a nanomaterial it is necessary to use alternative methods like acoustic spectroscopy or dynamic light scattering. In this study, acoustic spectroscopy was preferred in order to measure the sample in its original concentration and dispersed conditions. This would not be possible with dynamic light scattering due to the necessity of diluting the sample to a minimum.

Acoustic spectroscopy

Acoustic spectroscopy provides a promising technique in order to characterize the present particle mixture here accurately due to its lower limit of 5 nm. The DT-1202 from Dispersion Technology was used for the experiment. Figure 4 shows the volume based particle size distribution of the composition.

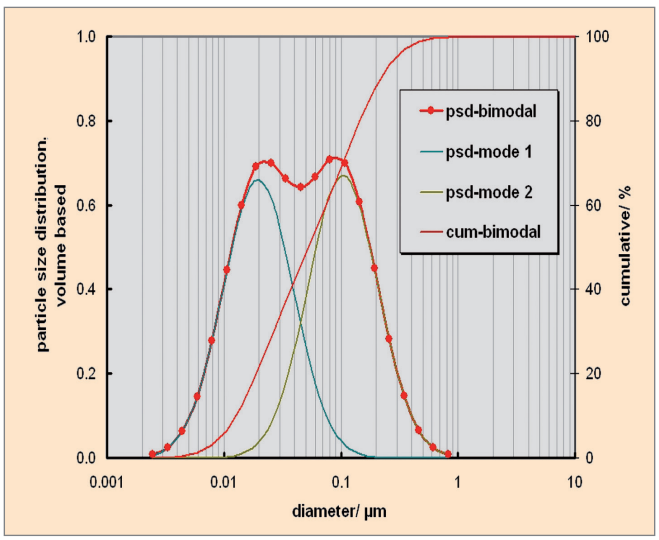

Figure 4 *Particle size distribution of the mixture of silica 1 and silica 2 (50/50) carried out with acoustic spectroscopy (volume based)*

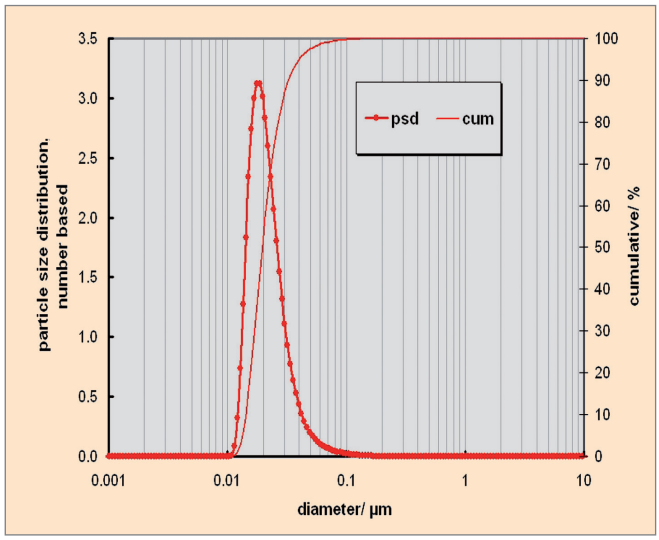

Figure 5 *Particle size distribution of the mixture of silica 1 and silica 2 (50/50) carried out with acoustic spectroscopy (number based)*

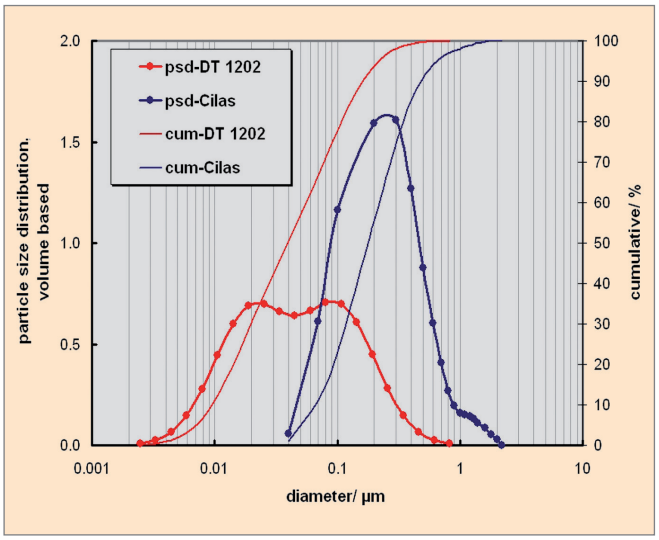

Figure 6 *Comparison of measurement techniques acoustic spectroscopy and laser diffraction for a silica mixture (volume based)*

The result is a bimodal size distribution. The recovery of the used materials is very good regarding to the particle size and the masses. The instrument can separate the two fractions very well, though the size distributions overlap in the middle area. The determined number based size distribution shows (see figure 5), that this distribution is dominated by the particles of the small fraction (silica 1). The bimodality can only be assumed by the slight asymmetry of the distribution.

In comparison with the results of laser diffraction it can be seen that most of the detected particles are below the official lower limit of 40 nm for the laser diffraction method. This is the reason for wrong results in the laser diffraction experiment. Figure 6 shows an overlay of the two different sizing methods to characterize the size distributions of the silica composition.

Conclusion

QUANTACHROME offers a number of instruments based on different methods to characterize entirely varying particulate systems. Especially for the low nanometer range, several methods get to their lower limits of accuracy. On the one hand the experiment in this study should present two methods which could be helpful to separate materials in "nano" or not. On the other hand the following problem should be pointed out: With the choice of the wrong method, a complete particle fraction of a mixture of powders could be ignored. This can lead to misinterpretation regarding to the question of classification in "nano" or not. In the given example, the complete fraction of silica 1 was not detectable with the laser diffraction instrument, though the quantity of these particles represents more than 95 % of the sample. To avoid this problem, a different method with other lower limits has to be used.

Furthermore, particle size distribution is not the only important parameter to characterize a nanomaterial and its properties. Zeta potential for information about the ability of agglomeration or surface area as a parameter for particle shape or pore structure should be mentioned as well.

References

[1] *Günter Schmid, Benedetto Corain: "Nanoparticulated Gold: Syntheses, Structures, Electronics, and Reactivities.", European Journal of Inorganic Chemistry, 17, 2003, 3081–3098*

[2] *http://www.scribd.com/doc/49647550/schmelzpunkt-gold accessed on 2012-02-01*

[3] *http://europa.eu/rapid/pressReleasesAction.do?reference=IP/11/1202&format=HTML&aged=1&language=EN&guiLanguage=en accessed on 2012-03-13*

[4] *Hatch, T., Choate, S. P., J. Franklin. Inst. 207, 1929, 369-387*

[5] *QUANTACHROME, particle world 2, 2009*

[6] *QUANTACHROME, particle world 3, 2009*

[7] *Malitson, I. H., J. of the optical society of America 55 (10), 1969, 1205-1209*

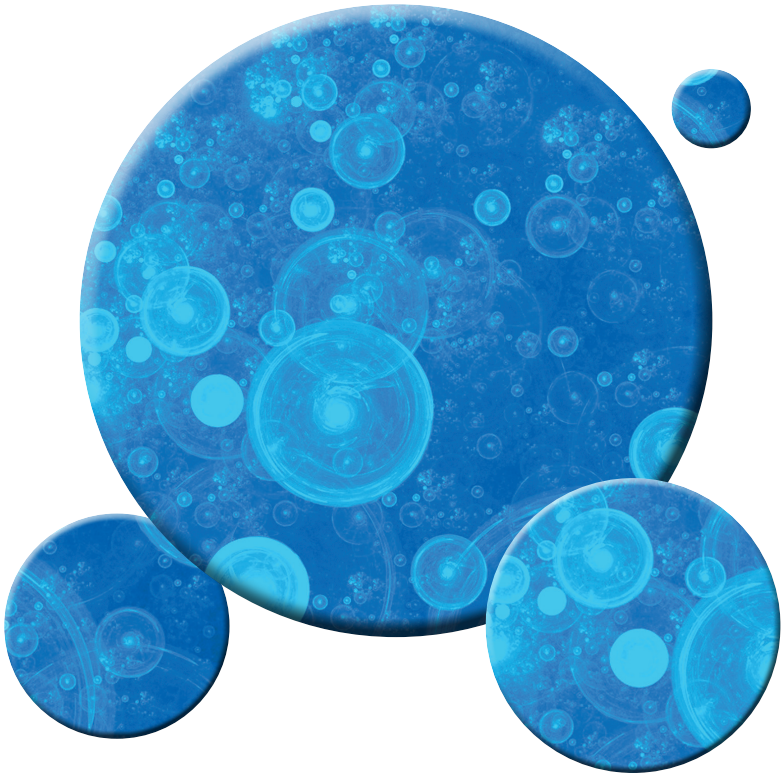

Figure 1 *GEOCHEM Ltd. – the start in the new building in 2009 (QUANTACHROME's POREMASTER, AUTOSORB and PENTAPYC in the meantime in the GEOCHEM lab, instead on the contruction sign building blackboard)*

GEOCHEM – the partner of QUANTACHROME for Hungarian customer support – developed a new instrument for high pressure permeability analyses of geological samples

Dr. Ferenc Fedor, *GEOCHEM Ltd., fedor.ferenc@geochem-ltd.eu*

The petrophysical laboratory of our company (Figure 1), GEOCHEM Ltd. is working since 2009 in Kövágószölös, near Pécs (S-Hungary), constantly developing its services to meet the expectations of its customers. The main activities are the characterization of pore structure and permeability of various rock types and related research and development. Our references are connected to this field of geology, mainly to the disposal of radioactive waste (LLW-ILW, HLW) in geological environment, petrophysical measurements related to geothermal research and special measurements connected to hydrocarbon and coal exploration. The particular focus is on the investigation of border areas, namely on the measurement of very tight and unconsolidated rocks. The laboratory possesses all equipments that are needed for the formation of small cores (plugs) from rocks. Our speciality is the preparation of 9 mm plugs, important for pore structure measurements. In most cases measurements are performed on regular plugs with 1-1.5" diameter and of max. 3" length (Figure 2), but instruments are also suitable for the measurement of debris and powder samples. During sample preparation distilled water or air is used for cooling, to avoid the contamination of samples.

The pore structure laboratory is the reference laboratory of QUANTACHROME GmbH & Co. KG in Middle Europe since 2009. It is equipped with a Quantachrome Pentapyc 5200e helium pycnometer, containing a cooling and heating thermostat, with a QUANTACHROME Autosorb-1-MPV physisorption instrument (suitable for vapor sorption measurements as well) and with a QUANTACHROME Poremaster 60 GT mercury porosimeter, containing two small pressure ports for preparation and measurement and two high pressure measurement ports. The exact knowledge of the sample's geometry and the measurement of its mass with an analytical scale make possible the determinination of matrix volume, as well as rock density, specific density and porosity. An uncertainty parameter is assigned to every measurement, including He-porosity as well. In the majority of projects, this is a basic requirement from the customers. The advantage of the investigation of cores with 9 mm diameter and regular geometry is that it is possible to perform He-pycnometry measure-

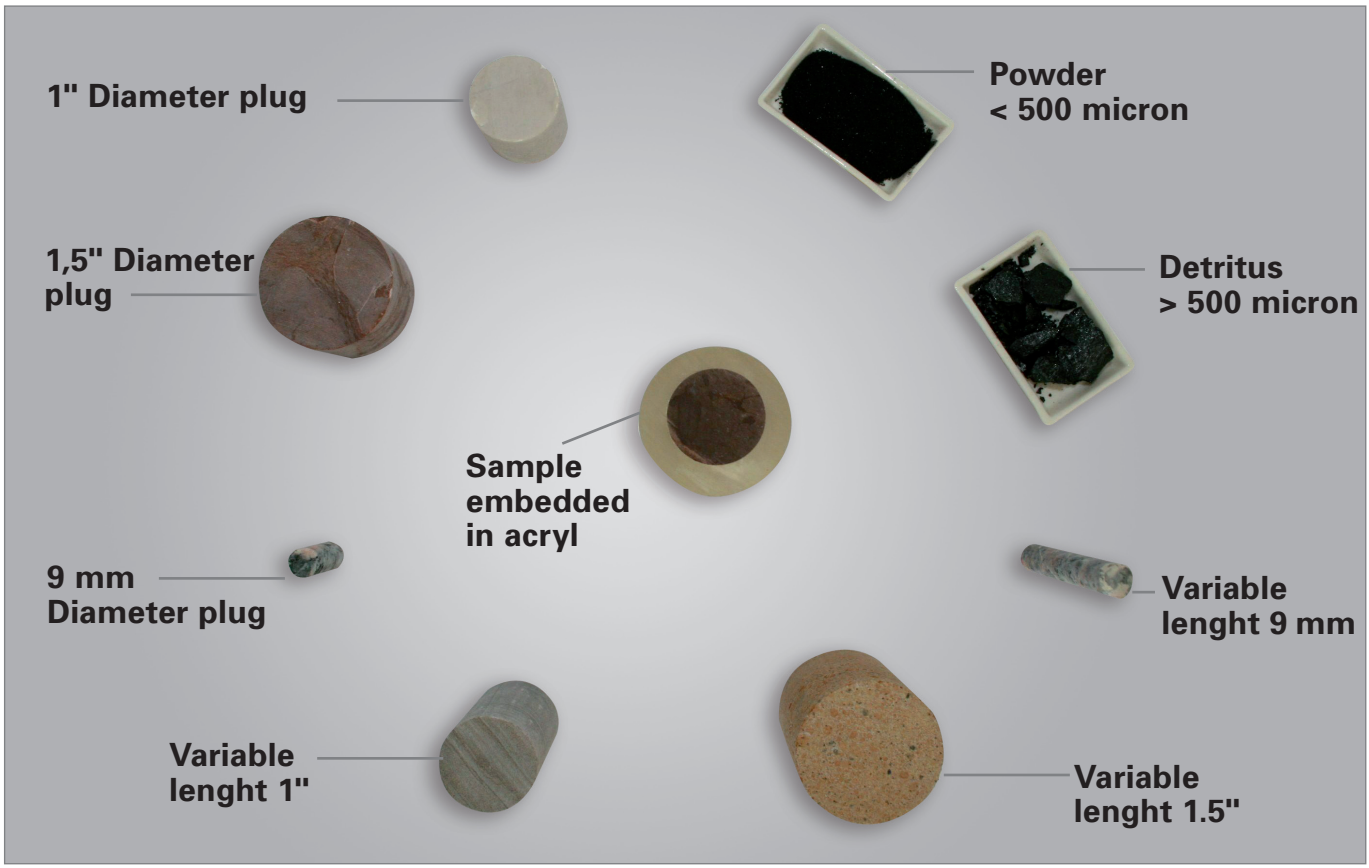

Figure 2 *Typical geological samples, prepared at GEOCHEM for pore characterization measurements*

ment, to characterize micro- and mesopore and afterwards to measure Hg-porosimetry without material loss and other representativity problems, that means, we get the complete pore structure of the given plug. With Autosorb-1-MPV instrument we mainly use nitrogen and carbon-dioxide. Before mercury porosimetry measurements, contact angle is always measured with a QUANTACHROME contact anglometer on the material identical with the sample. Our experience is that measuring contact angle can significantly influence interpretation, especially in the case of materials with mesopore structure.

After drying and He-pycnometry we perform permeability measurement on 1 and 1.5" core samples, using the self-developed RS-PPD-01 universal permeameter (Figure 3), either with gas or liquid. This instrument is universal, because it is suitable for steady-state and transient measurements with gas and liquid as well. At present, the maximum confining pressure (lithostatic pressure – radial pressure on the core mantle) is 350 bar, max. pore pressure is 320 bar, max. temperature is 150 °C and pressure difference between the two sides of the rock can be varied between 0.01-30 bar. In practice, this means reservoir conditions equivalent to 1500-1800 m depth. We are continuously working on the further development of the instrument and of its likewise self-developed program. With the instrument it is possible to measure permeability to nanodarcy-pikodarcy range, in a relatively short period of time (1-3 days). Liquid permeability is usually measured with self-prepared ultra clean water, but besides this, there can be used acid and alkaline solutions too.

Our company places great emphasis on environmental consciousness (environmental management system) and on the safe management of data. All information about different measurements and interpretations are stored digitally. Since July 2011, GEOCHEM Ltd. provides the Hungarian service for instruments and other devices from QUANTACHROME GmbH & Co. KG and participates in sales. Measurement services can be ordered through QUANTACHROME or directly at GEOCHEM Ltd. The cooperation agreement between the two companies expectedly opens new possibilities for further common development projects in investigating rock reservoir characteristics. You can find more information about the developments and services on the following website: **www.geochem-ltd.eu**.

Figure 3 *Self-developed RS-PPD-01 universal permeameter from GEOCHEM Ltd.*

The DISPERSER QC –

the dispersion unit in connection with external analyzers

Sampling, sample splitting and sample preparation are essential basics for the later analysis results and further interpretations regarding the quality of a raw material, intermediate- and end products. Sample splitting, especially from coarse objects or particles with wide particle size distribution, is often necessary after sampling. For the analysis of bulk and other coarse goods with the ZEPHYR analysis system (Figure 1) and sample requirements of ca. 0.2 – 2 kg a previously performed sample splitting with the QUANTACHROME SIEVING RIFFLER (Figure 2, left) can be advantageous, e.g. if the sample has to be taken out of a big pile. As the required sample quantities for many other analyzing methods or for standard sample cells are substantially smaller and in the lower gram range, small but representative sample quantities can be obtained in using a QUANTACHROME MICRO RIFFLER for sample splitting.

Figure 1 *ZEPHYR analyzer for the determination of particle size and shape distribution of bulk materials (granulates and powders) by means of fully automated shape analysis*

Figure 2 *QUANTACHROME sample splitting devices: SIEVING RIFFLER (left) and MICRO RIFFLER (right)*

The sample preparation of representative samples, obtained by sample splitting or ready to use, includes in case of liquid measurements the stirring of particles and dispersing agents (if the material is further processed in suspensions), the application of ultrasound for the dispersion of the particles resp. for redispersion of agglomerates, the injection of liquid dispersions to the sample cell of the analyzer and the recirculation of the dispersion from the sample cell.

The liquid dispersion of CILAS lasergranulometers excels by integration of optimized stirring, ultrasonic treatment of liquid dispersions and the injection and rinsing systems and is the basis for exact analysis results with outstanding reproducibility. These components are

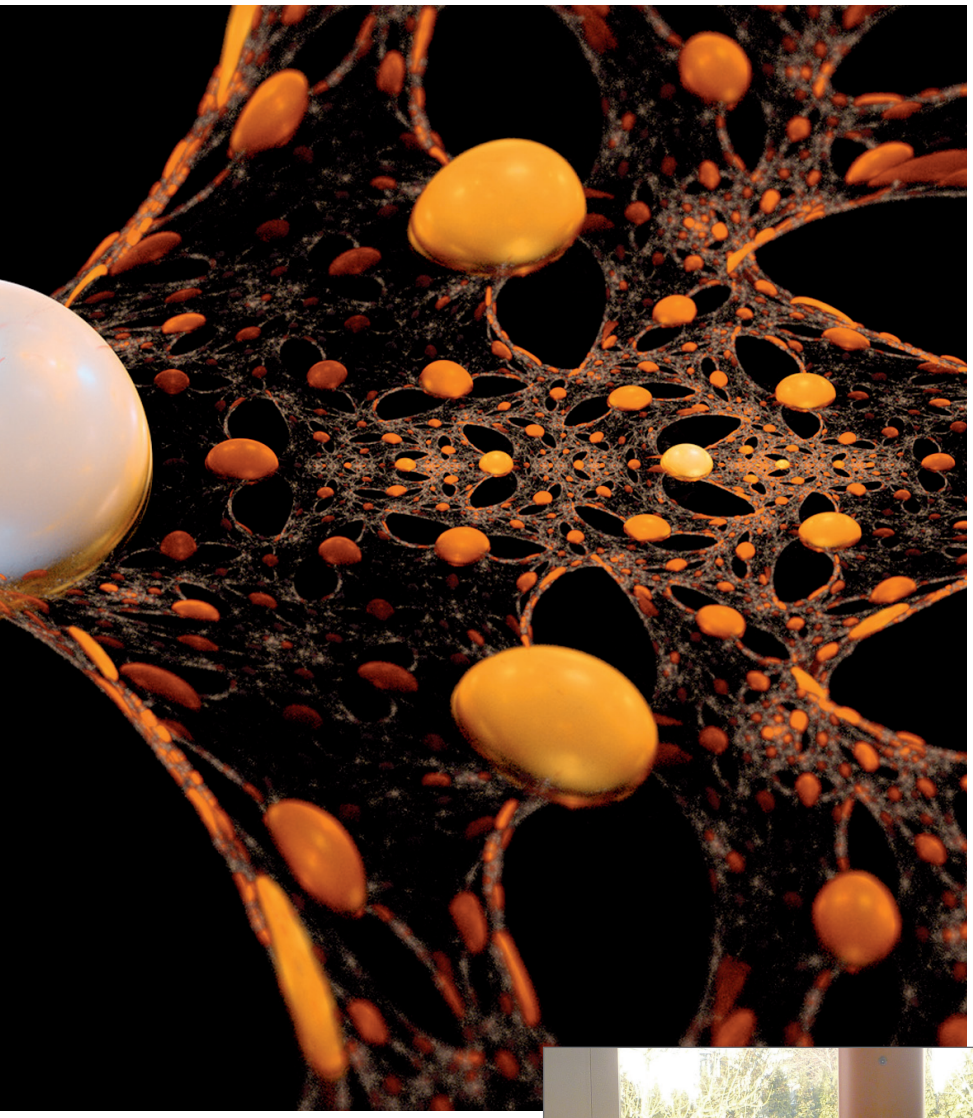

Figure 3
DISPERSER QC2 – the external dispersion unit with integrated stirrer, ultrasonic bath and circulation pump system is combinable in principle with any analyzer for the characterization of suspensions, front view (below) with peristaltic pump, display and operating buttons and plan view (above) with ultrasonic bath and stirrer

already integrated in CILAS lasergranulometers and can be further optimized, e.g. with a sonotrode for injection of larger dispersion energies. Dispersion units are not always integrated in other analyzers as for certain tasks they are not useful at all or only in adapted version. QUANTACHROME has developed for this reason a separate dispersion unit which can be combined with other analyzers. Thus the connection of the DISPERSER QC (Figure 3) is easily possible with OCCHIO analyzers for particle size- and –shape analysis of liquid dispersions, with the EXPERT SHAPE option of CILAS as stand-alone version for particle shape analysis, as well as dispersion option for the particle size and zeta potential analyzers of DISPERSION TECHNOLOGY.

New WAVE analyzer series for the characterization of porous materials in regard to porosity, pore size and zeta potential

The quick determination of porosity as well as of the average pore size is required for the solution of many tasks. Traditional gas adsorption and mercury porosity methods as well as the capillary flow porosimetry for the measurement of through (filter)-pores are available therefor. QUANTACHROME offers with the new devices of the WAVE series (Figure) pore analyzers which do without mercury, liquid nitrogen as well as without vacuum pumps or high pressure systems. Besides the determination of porosity and the average pore size also the characterization of the zeta potential of porous structures is possible with the new WAVE analyzers. Table 1 points out their analysis possibilities, table 2 shows the specifications in regard to the parameters to be determined.

Table 1 *Measurement possibilities of the analyzers WAVE 1905, WAVE 2305 and WAVE 3805*

	Porosity [%]	Average pore size [nm]	Zeta potential porous materals [mV]
WAVE 1905	yes	**no**	**no**
WAVE 2305	yes	**no**	yes
WAVE 3805	yes	yes	yes

The basic method for the determination of the average pore size by electroacoustic spectroscopy is the so called seismo-electric effect. An electrochemical double layer at the pore walls forms due to the saturation of a porous material with a polaric liquid. An induced ultrasonic wave shears off the diffuse layer in the double layer. A potential difference develops at this shearing surface, which is detectable as oscillating current. The pore-zeta potential gets determined out of this signal. A saturation with non-polar solvents causes the double layers to overlap in the pores. The seismo-electric current depends on the pore diameter in this case. A patent is filed for this method (A1 2011 0283800 „Method for determining porosity, pore size and zeta potential of porous bodies“).

The determination of the percentage porosity is based on very high-frequency (MHz-range) conductivity measurements. The porosity of all pores gets analyzed with the high-frequency method, thus not only of through pores and connected pore-networks but also of the so called blind pores with only one pore access, which is different to normal conductivity measurements. The Maxwell-Wagner theory brings the relation of the conductivities of pure solvent and saturated porous material in connection with the porosity of the material. Also this method has been filed for patent (A1 2011 0012627 „Method for determining porosity with high frequency conductivity measurement“).

Table 2 *Specifications of the WAVE-series in regard to average pore size, porosity and zetapotential*

Average Pore Size	**WAVE 3805**
Analysis principle	Electroacoustic spectroscopy (seismo-electric effect)
Average pore size	ca. 10 nm bis > 5 µm
Repeatability	< 1 %
Porosity	**WAVE 3805, 2305, 1905**
Analysis principle	Conductivity (at very high frequencies in the MHz-range)
Resolution	0,5 %
Accuracy	< 10 %
Repeatability	< 1 % absolute
Conductivity	0,001 – 10 S/m, ± 1 %
Pore-Zetapotential	**WAVE 3805, 2305**
Analysis principle	Analysis principle Non-isochoric streaming current (seismo-electric effect)
Measurement range	± 0,5 % mV, no upper + or - limitation
Resolution	± (0,1 + 0,5 %) mV

Fields of application

No fundamental limitations are basically to the applications for the WAVE methods and analyzers as long as the materials are insolvable in the according liquids and the parameters to be determined are within the scope of specifications (table 2). Various ceramics, drilling cores of geological samples or building materials, silica and other high porous materials, resins, tablets, brake linings, battery components and many others are accordingly typical applications.

Every user can choose the WAVE analyzer matching the specific tasks because of the modular concept. While the WAVE 3805 enables with the analysis of average pore size, pore zeta potential and porosity the determination of three parameters with one analyzer, only the measurement method for very rapid evaluation of porosity (without mercury) is implemented in the WAVE 1905.

Analysis possibilities for all three parameters (porosity, average pore size and pore zeta potential) are available in the LabSPA (Laboratory for scientific particle analysis) for test and contract analyses as well as for method developments (e.g. evaluation of the relevant parameters to replace other methods).

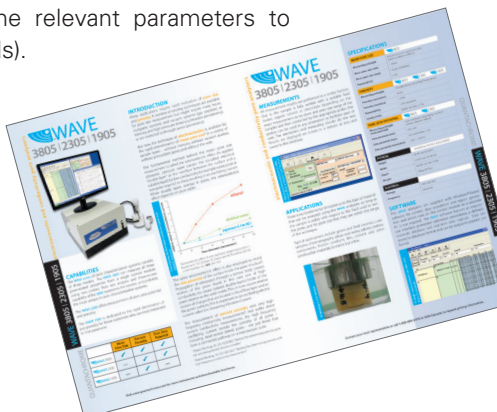

Figure *Brochure to the new WAVE series (3805, 2305 and 1905) for the characterization of average pore size, porosity and zeta potential of porous materials*

Determination of specific surfaces of different dimensions

Dr. Dietmar Klank, dk@quantachrome.de, www.quantachrome.eu.com

Introduction

The porosity and the specific surface of solids and powders play a decisive role in many natural and industrial processes. Geological changes, ageing processes and rates, catalytic activities or separation behavior of solids depend mostly as much on porosity and surface consistence as the reactivity, solubility and the sintering behavior of powders do. In the scope of analytical methods it is left undecided if, in the individual case, these processes are favored or not. The determination of surface and pore structure can lead to significant insights regarding the understanding and optimization of processes.

The specific surface of nonporous powders depends on their degree of fineness. Out of a particle size analysis it is also possible to assess the specific surface area if the density is known and a particle geometry is presumed. However, the standard method for the determination of the specific surface area of porous solids and powders is the gas adsorption method. Out of this method results the value for the specific area of all open pores including the external surface. In this article the basics, analysis options and results out of particle size and gas adsorption measurements as well as alternative measurement conditions for certain measurement tasks will be described.

Analysis method

If the surface of a solid is brought into contact with gas molecules, parts of them accumulate at the surface. This accumulation of molecules is called **adsorption**, the solid **adsorbent**, the sample gas **adsorptive gas** and the adsorbed phase as **adsorbate**. If this process is based on unspecific (physical) interactions (e.g. van der Waal's interactions) it is called **physisorption**. The physisorption is a reversible and dynamical interaction which can be stimulated in lowering the temperature as it gets intensified with increasing relative gas pressure p/p_0. The reverse process – the elimination of adsorbate molecules from the surface (**desorption**) - is endothermal, the supply with energy can result, for example, from the increase of temperature. With the desorption one is confronted mostly already before the measurement actually starts. To be able to measure a pure surface, external molecules - e.g. in the form of lubrication - have to be removed from surface and pores. This endothermal desorption of water and other molecules is in most cases executed in vacuum at increased temperatures.

If an adsorbent-adsorbate-system is in a dynamical sorption equilibrium it means, that the amount of ad- and desorbed species per time unit is the same. The adsorption equilibrium can be described with the adsorption isotherm

$$\Theta = f(p)\ ;\ (\text{temperature } T = \text{const.}) \qquad (1)$$

with the surface coverage Θ respectively the adsorbed gas amount, at constant temperature T, which depends on the pressure p respectively the **relative pressure p/p_0**. The adsorbed gas amount as function of the pressure at constant temperature leads to pairs of variates which form the sorption isotherm. With the enhancement of pressure the surface gets increasingly covered with gas molecules. Simplified one can imagine that at a certain pressure a **monolayer** of gas molecules forms at the solid surface. By continued adsorption at higher pressures the development of further layers and a pore filling process (**capillary condensation**) result, whereat a direct dependency of the pore diameter from the relative pressure is given. At pressure reduction gas molecules get removed from the solid surface, and at this process the dependency of the solid charging from the equilibrium pressure can be analyzed as well. In the scope of the gas sorption there are different methods to measure the adsorbed gas amount, essential ones are outlined in the following.

Figure 1 *Static-volumetric analyzers for BET surface area and with additional options for pore analysis and high sample throughput /1/*

(from the left: QUANTACHROME AUTOSORB-iQ, NOVA, QUADRASORB SI)

- **Static-volumetric method:** a sample in a vacuum gets dosed with a certain gas amount. The determination of the adsorbed gas amount is based on a gas equation and is executed by pressure measurements in volume calibrated systems.
- **Dynamic method:** a mixture of analysis and inert gas overflows continually the solid until the adsorption equilibrium is reached. The difference in the gas consistency caused by adsorption is captured by a heat conductivity sensor.
- **Gravimetric method:** the determination of the adsorbed gas amounts results from differential weighing of the sample before the dosing and after reaching the sorption equilibrium.

BET surface area

Brunauer, **E**mmett and **T**eller developed an equation in 1938 with which the necessary gas amount V_m for a monolayer on the solid surface can be calculated out of gas adsorption analyses. Model assumptions of the BET-method are /2/

- localized adsorption
- multilayer adsorption
- homogeneous solid-surface (similar adsorption centers cause similar energetic interaction)
- the adsorption enthalpy of the first layer is independend of the solidity ratio
- the adsorption enthalpy of the further layers are in accordance with the condensation enthalpy of the adsorptive
- no interaction of the adsorbate molecules in a layer.

By use of the BET-equation the amount of adsorbate that forms the monolayer is calculated out of the adsorption isotherm respectively out of the very part of the isotherm which lies in the extent of validity of the model assumption. The BET-equation

$$V_a = V_m \frac{Cp/p_0}{(1-p/p_0)(1-p/p_0+Cp/p_0)} \qquad (2)$$

gets traditionally interpreted in its linearized form:

$$\frac{p/p_0}{V_a(1-p/p_0)} = \frac{1}{V_m C} + \frac{C-1}{V_m C}\frac{p}{p_0} \qquad (3)$$

In the diagram the term p/p_0 gets displayed on the x-axis and the term $(p/p_0)/(V_a(1-p/p_0))$ on the y-axis. V_a is here the adsorbed gas amount at relative pressure p/p_0, V_m the monolayer capacity looked for and C the so-called BET-constant.

The interpretation procedure becomes evident in figures 2 to 4. Analyzed gets a more or less complete isotherm (fig. 2). If only the BET-surface area is searched for, measuring points in a certain relative pressure area are of sufficient significance, therefore not the complete isotherm has to be analyzed. If for the whole adsorption isotherm (fig. 2) a BET-analysis is made this leads to fig. 3. At relatively low pressures a straight line – section is recognizable, while the BET-plot at higher relative pressures leads into a hyperbola shaped graph. Differences to the straight line are interpreted as deviations to the BET-model. Therefore the calculation of the BET-surface is effected only within the extent of validity of the BET-equation, i.e. in the straight line range of the BET-plot as to see in fig. 4.

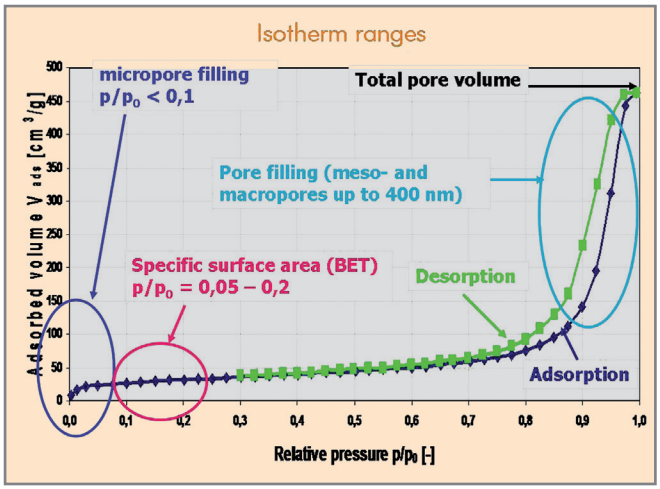

Figure 2 *Adsorption and desorption isotherm of a mesoporous solid*

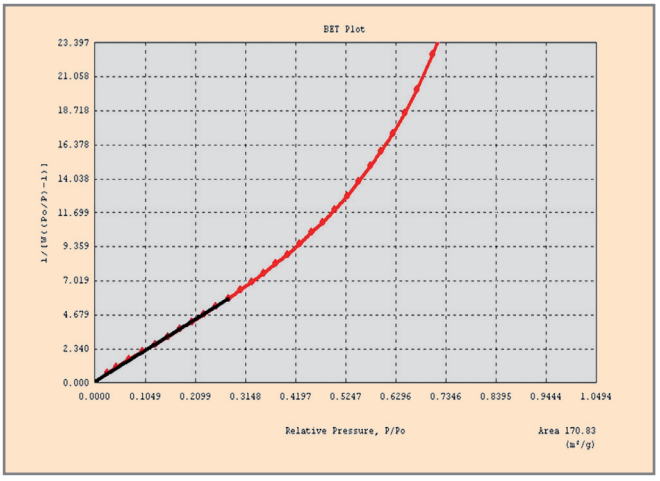

Figure 3 *BET interpretation of the complete adsorption and desorption isotherm of figure 2*

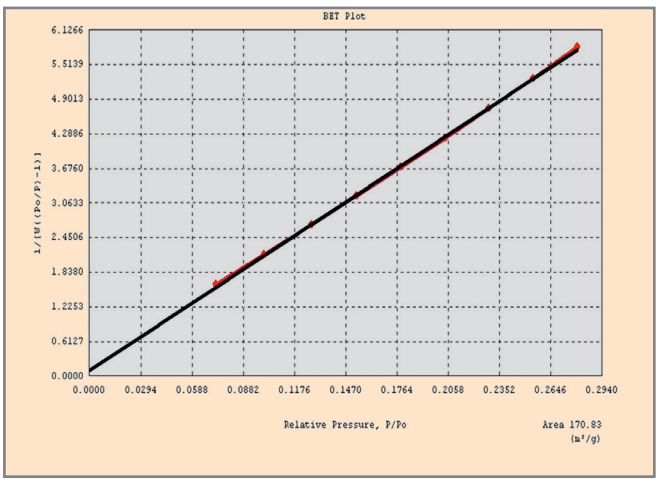

Figure 4 *BET straight line of the isotherm, the interpretation is limited to the extent of validity of the BET-equation*

From the linearized BET-equation the slope s and the intcept i are gained. The monolayer capacity results from

$$V_m = 1/(s + i) \quad (4)$$

and the BET-constant C from

$$C = s/i + 1 \quad (5)$$

At the recalculation of results it has to be considered that the volumina contained in the equations above can be written also as adsorbed masses or adsorbed moles. Correct use of the adsorbed gas volumina, mass and mole quantities leads to the monolayer capacity. If this monolayer capacity V_m is displayed as quantity of substance in mol, the product received with the Avogadro constant is the amount of in the monolayer adsorbed molecules and with the space of one adsorbate molecule am the specific surface O_{sp}.

$$O_{SP} = V_m \cdot N_A \cdot a_m \quad (6)$$

The extent of validity of the BET-equation is usually between p/p_0 = 0.05-0.3 and is limited downward by the influence of energetic surface heterogeneities, upward by the influence of capillary condensation.

The BET-constant C of the BET-equation is approximately

$$C = e^{(q_1 - q_L)/RT} \quad \text{resp.} \quad q_1 - q_L = RT \ln C \quad (7)$$

whereat $(q_1 - q_L)$ is the net heat of the exothermal adsorption process; however, it is explicitly pointed to its approximative character. If the adsorption heat of the first adsorbate layer changes with the surface coverage Θ_1 the C-value deviates from equation (7).

The net heat of the adsorption of a sample gas depends on the solid respectively on the interaction between gas and solid. The C-constant determines the initial range of the adsorption isotherm shape. The larger the BET-constant C the steeper continues the initial area of the adsorption isotherm, the smaller the BET-contant C the more the initial area proceeds along the x-axis (relative pressure axis). Analyses on the same material should lead to same or similar C-values.

The procedure for the determination of BET surface areas by means of gas adsorption is described closer in ISO 9277 /3/.

Surface areas determined by use of different sample gases can deviate from each other, especially because of approximated physical parameters for each adsorptive. Nitrogen measurements at 77.4 K are traditionally applied for the determination of the specific surface and are for many cases the only basis for a comparability of BET results.

The BET-assumptions are theoretically not valid for isotherms of the so-called type I, i.e. not for microporous solids, but strictly seen only for isotherms of the type II (nonporous or macroporous solids) and the type IV (mesoporous solids). However, after a long discussion there is an appendix in ISO 9277 now which describes a procedure how to use the BET equation for the calculation of microporous surface areas. The author very much appreciates that compromise, because he calculated BET surface areas of microporous active carbons for a long time and sees the recent compromise between theory and practice in the ISO 9277 norm as the most important step towards comparable BET surface area data for the microporous solids from different laboratories in the future.

Specific surfaces established by means of particle size distribution and BET-method

If there is the opportunity to determine the particle size distribution with an automatic analyzer it is possible to assess the specific surface out of the particle size distribution. Here it is agreed on the assumption, that all particles are spherical (or do have a certain form factor) and nonporous. Examined were different powders (table 1 and 2), building materials, foods, titania, graphite and others. The particle size analyses were made with the laser particle sizer CILAS 1090 L (table 1) and, for nanoparticles, with the acoustic spectrometer DT-1201 (table 2). The density measurements were executed with the ULTRAPYC 1200e T by use of helium, the BET surface areas were calculated from nitrogen adsorption measurements at 77.4 K with the NOVA 2200e, i.e. analyses between p/p_0 = 0.05 - 0.25. The milk powder was examined with the AUTOSORB-iQ by use of krypton adsorption at 77.4 K.

The data in table 1 show that the very part of the geometric surface, which was analyzed by a spherical particle model

Table 1 *Surfaces of different powders in the micrometer range out of partice size distribution and the BET-method*

	Particle Size [µm]			Density [g/cc]	Surface area [m²/g]		
	D10	D50	D90		geometric	BET	F = BET / geometric
Cement	1.11	8.70	26.8	3.02	0.72	1.75	2.4
Lime	0.95	5.51	29.4	2.74	0.92	1.41	1.5
Filler material	1.18	6.99	41.6	2.38	0.96	1.04	1.1
Silica gel	21.50	84.20	121.6	2.30	0.07	114.00	1628
Titania	0.76	3.31	9.39	4.23	0.89	51.09	57.0
Zinc oxide	0.42	1.26	4.77	5.60	1.23	5.33	4.3
Graphite	1.43	9.74	22.4	2.27	0.81	10.71	13.0
Lactose	3.50	24.10	59.8	1.58	0.55	1.36	2.5
Milk powder	23.10	58.20	94.2	1.73	0.22	0.26	1.2

Table 2 *Surfaces of different powders in the nanometer range out of partice size distribution and the BET-method*

	Particle Size [µm]			Density [g/cc]	Surface area [m^2/g]		
	D10	D50	D90		geo-metric	BET	F = BET / geometric
Silica	19.9	28.0	36.60	2.17	98.7	161.1	1.6
Alumina 1	17.6	27.1	43.20	3.05	72.6	145.7	2.0
Alumina 2	13.0	21.9	32.13	3.01	91.0	207.1	2.3
Carbon black	105.2	146.7	206.90	1.82	22.5	65.3	2.9

without form factors, diversifies strongly at the BET surface (see last column). At the examined building materials, foodstuffs and zinc oxide the differences are explainable in regard to the surface roughness. Plate-shaped graphite particles cause substantial differentials because of the difference of their particle shape. While the calculations based on the particle size assumed spherical particles, flaky graphite particles were analyzed with the BET method. Even stronger deviations are shown at porous solids as titania and silica gel.

It shows at the examined nanoparticles that their large specific surfaces result only out of the very small particle diameters. These large BET-surfaces render a possibility for the characterization of nanoparticles. Thus the standard BET-analysis of surfaces presents an outstanding alternative to obtain information about the degree of fineness of nanomaterials.

Determination of very small surfaces

In general large surfaces are more precisely measurable than very small ones as stronger adsorption effects more distinct measuring signals. This applies particularly if only few sample material is available. Essential for the analysis of smaller specific surfaces is the matter of the so-called 'free space volume' or 'dead volume' of the measuring system, i.e. the volume in which the sample reach the adsorption equilibrium. The adsorbed gas amount gets determined in waiting until the sorption equilibrium with minimal changes in pressure respectively constant pressures is reached. Afterwards the not adsorbed gas, which remains in the equilibrium system, gets subtracted from the dosed gas amount. The larger the difference between dosed and not adsorbed gas amount at an analysis, the higher is the relative change in pressure within the measurement system compared with the change of the pressure in case of a blank run (measurements without sample).

If sufficient sample material is available the weighted sample should be maximized to reach wider measurement effects. Yet how can the free space volume respectively the amount of gas molecules in the system volume be reduced? Please find in the following possibilities for this:

1. Use of sample cells with small volume: therefor the possibilities of manufacturer and user are almost unlimited. The usage of a filler rod optimizes the measurement conditions.

2. Use of a small manifold (dosing volume): The dosing volumes of the analyzers are mostly optimized. Large manifold volumines can dose large amounts of gas but maybe are less sensitive regarding small alterations of the gas amount. Otherwise a too small manifold volume makes necessary many dosages for each measuring point and should be avoided.

3. Separation of the dosing volume from the sample cell volume after the gas dosing: A distinguishing feature of the AUTOSORB-iQ from QUANTACHROME is, that not the complete manifold is part of the measuring volume during equilibration. With this separation of a part of the manifold during equilibration both the relevant free space volume becomes significantly reduced as well as the relevant leakage rate for the sample can be minimized.

4. Cooling down to measurement temperature only of the relevant part of the sample cell: The AUTOSORB-iQ realizes by means of a thermistor principle that only the sample gets cooled with liquid nitrogen and not the sample stem as well. Reason for this is that at e.g. 298 K and constant pressure per volume cold zone there are exactly 298 K / 77 K = 3.87 times more molecules than in the according warm zone at 298 K. This means that the reduction of the dead volume in the cold zone of 1 cm^3 is equivalent to a reduction of the free space volume in the warm zone of 3.87 cm^3.

5. Measurement at low pressures: As the scope of validity of the applied analysis methods is given respectively results out of the adsorption mechanism only alternative sample gases offer influence. By use of sample gases with lower saturation vapor pressure lower pressure areas can be reached which is shown in figure 5.

Figure 5 shows the dependency of the saturation vapor pressure from the temperature of the sample gases nitrogen, argon and krypton. From the boiling temperature of the liquid nitrogen (x-axis at 77 K) a saturation vapor pressure for nitrogen of ca. 100 kPa (ca. 750 mm Hg), thus close to ambient pressure, can be read from the y-axis. At the same time it shows that at higher temperatures the saturation vapor pressure increases significantly. At a temperature of 84 K the saturation vapor pressure of nitrogen amounts already to twice the ambient pressure (200 kPa resp. 1500 mm Hg). At this temperature an isotherm can not be analyzed anymore to its saturation vapor pressure with a normal pressure apparatus.

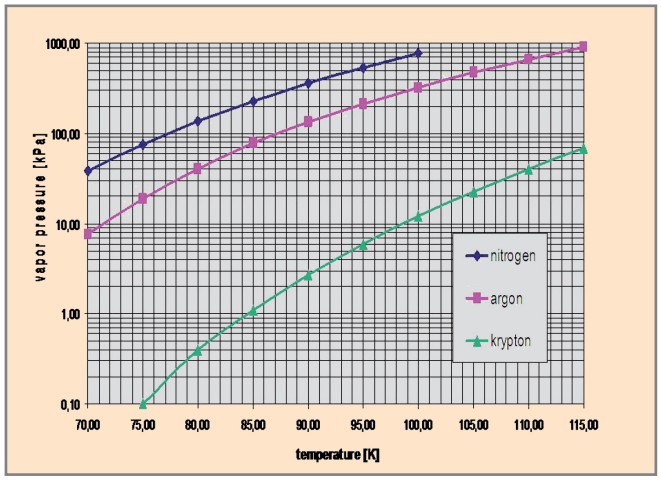

Figure 5 *Saturation vapor pressure of nitrogen, argon and krypton depending on temperature*

It also shows for argon that the saturation vapor pressure at the argon boiling temperature of 87 K is about 100 kPa (750 mm Hg). The measurement of an argon isotherm at 87 K is therefore well possible with a commercial sorption apparatus and is recommended for micropore characterization. Yet how does the saturation vapor pressure of argon change if liquid nitrogen with 77 K is used for tempering? As this ranges below the boiling temperature of the measurement gas the saturation vapor pressure lies below the ambient pressure as well. In the case of argon at 77 K the saturation vapor pressure is about 30 kPa (220 mm Hg). Therefore it can be concluded that in case of the argon adsorption at 77 K, in contrast to nitrogen adsorption at 77 K, only less than 1/3 of the number of molecules are in the free space volume available during a measurement. If the given sample adsorbs a certain amount of gas molecules then the sensitivity of the argon adsorption should be higher for the factor 3. This positive effect becomes particularly relevant at small surfaces, i.e. at the measurement limit of the analysis method, and can be intensified if the saturation vapour pressure gets further lowered. Figure 5 shows this for krypton. At 77.4 K the saturation vapour pressure of krypton is only about 0.2 kPa (2.6 mm Hg). If a small surface adsorbs a certain amount of molecules the change of pressure is higher if the adsorption results out of a small amount of gas. At such a low saturation vapour pressure of krypton as 77.4 K both the quantity of molecules diminishes and the sensitivity of the measurement increases many times over. Because of the low pressure at krypton adsorption at 77 K only about 1/300 of the molecules are in the free space volume compared with nitrogen measurements. Thus krypton is used successfully for the determination of very small surfaces (< 0.5 m^2). The minimally necessary surface area in the sample decreases from about 0.5 m^2 for nitrogen to well below 0.05 m^2 for krypton measurements with the AUTOSORB-iQ.

However, analyses at such low pressures require more powerful vacuum systems (turbo molecular pump) and additional low pressure transducers. The resulting disadvantage of higher costs must be tolerated if the determination of small surfaces is necessary and another solution is not practicable because of small sample quantity or small specific surface area.

Single-point BET method

When measuring only one volume-pressure-pair of values (single-point BET) a more or less substantial systematic error results out of it because of the postulate that the straight line runs through the point of origin. The analysis equation gets simplified for the BET single-point method to

$$V_m = V_a\left(1 - \frac{p}{p_0}\right) \qquad (8)$$

This simplified BET equation does not contain the BET constant C anymore. The single-point BET surface is therefore independent of this constant but cause a systematic error now, that means a difference to the more accurate BET multi-point method results. The error goes back to the C-constant which is only to evaluate by multi-point measurements and is, e.g., for a C = 100 and a relative pressure of 0.3 about 2.3 %. Because of the solid dependency of the unknown BET constant C is it well comprehensible that it is not possible to state a generally valid error explanation for the BET single-point method. For a soil sample as an example a specific surface area of 3.954 m^2/g was determined with the BET multi-point method and on the other hand with the BET single-point method a specific surface area of 3.720 m^2/g at a relative pressure of $p/p_0 = 0.25$, which is a deviation of 6 %. So why single-point measurements are still applied despite the possibility of the more precise multi-point measurements? In the following essential reasons are listed:

- Making out differences in the specific surface area of samples is possible also with the single-point method.
- Both methods, single- and multi-point, allow reproducible results.
- No multi-point measurement can be performed faster than an optimized single-point measurement. This can especially be decisive during production controls which aim to optimize the production process by means of the evaluated surface area value.
- Although the difference in prices between automatic single and multipoint analyzers became less during the last years, single-point BET analyzers usually still have a lower price.

BET surfaces of microporous solids

A typical hint at the BET-analysis towards microporosity (pores smaller than 2 nm) of a solid is, beside the partly very large specific surface areas, a slightly curved hyperbola. This effects that the ordinate intercept, gained by linear regression, and therefore the BET constant C becomes negative. Because of negative C values which are not possible in principle because of physical reasons (see equ. (7)), the BET method has been seen as valid only for isotherms of the type II (unporous or macroporous solids) and the type IV (mesoporous solids) in the past. The BET-surface are as parameter for microporous solids gets mostly only disregarded if alternative suitable analytical methods with a practicable time frame are available. Among these is the analysis of more or less complete adsorption isotherms for the determination of micropore volume and micropore distribution. Yet what to do if activated carbon, zeolites or other microporous solids have to be characterized by preferably most simple and quite fast gas adsorption analyses? The answer of many producers and developers of such products, to which the author agrees, is that BET-surfaces get nevertheless determined, against pure theory and a few model assumptions of the BET-method. If there would not be the practice to determine BET-surfaces of microporous products the question would remain how such solids could be compared as simple and fast as possible. For isotherm measurements often either the quite expensive equipment is not at hand or they are just too time consuming. A further aspect is the habituation effect towards the parameter BET surface area. It may be assumed that samples with larger BET-surface show also a larger surface respectively a larger adsorption capacity at microporous sample rows independent of the meaning of the term surface in an atomic scale. So independent of theoretical problems with the BET assumptions for microporous solids the BET surface area has been determined for a long time already to be able to compare different qualities of microporous samples.

Recently the ISO norm group found an agreement too to implement the BET calculation method for microporous solids in the appendix of ISO 9277. In principle the way is the same which the author already has been used for more than 20 years for the calculation of surface areas of microporous solids as active carbons or zeolites. To apply only the linear part of the BET graph for the calculation prevents the use of the ranges of the deviations from the BET straight line which are not according the BET model and therefore should not be used for the BET calculation. In applying the range of the BET straight line with a high correlation coefficient also the C value becomes normally positive so that as well this theoretical C problem can be solved this way.

ISO 9277 describes a procedure employing the BET C-value to find the right range according to theoretical assumptions. Otherwise, from practical point of view, if the correlation coefficient of a straight line is very high, e.g. > 0.9999, the results do not depend significantly any longer if one data point less or more is taken into the calculation. However, for BET calculation of surface area of microporous solids, or better in general for all BET calculations, it should be informed together with the results also about the range of relative pressure for the BET calculation.

Please find in the following an example for the BET-interpretation in the general validity area and in the restricted range. Figure 6 illustrates for a microporous sample the shift in the analysis area. The generally valid area of the BET equation is marked with red arrows. The BET analysis of p/p_0 = 0.05 – 0.3 leads to a specific surface of 1009 m^2/g at a correlation coefficient of 0.9989. However, this refers to a linear calculation of a hyperbola. If one restricts for the examined microporous active carbon fibre the BET calculation to p/p0 = 0.01 – 0.08, a better straight line results out of it as is shown in figure 6 with black arrows. The BET calculation therefore results in a specific surface area of 1163 m^2/g at a correlation coefficient of 0.99999, which makes a difference of about 15 %. This point out that significant difference can arise only by different use of the BET-equation.

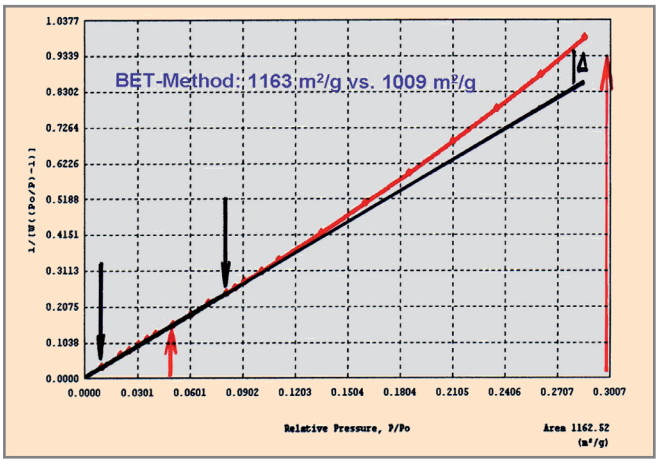

Figure 6 *Deviation of the BET straight line at high relative pressures*

Summary

The investigations show that surface evaluation out of particle size analyses only allow very limited conclusions on the actual surface for many powders. Roughness, deviations of the assumed spherical shape of the particles and especially the porosity are causes for the necessity to determine the BET surface area for the evaluation of samples. The krypton adsorption at 77 K makes it possible to determine also very small surfaces what can not be realized with the conventional nitrogen adsorption. For the characterization of microporous solids the practice and the ISO 9277 shows, despite theoretical inadequacies of the BET model for the adsorption in micropores, how a useful BET calculation can be done to compare samples qualities but also the results from different laboratories. The investigations point out that in any case it is preferable that technical lecture or data sheets indicate exactly how BET results were determined. Adsorptive and temperature, single or multipoint method as well as the used relative pressure range should be published.

Literature

[1] *Particle World 4, www.quantachrome.eu.com, p. 14*

[2] *Brunauer S, Emmett P. H., Teller E., „Adsorption of Gases in Multimolecular Layers", J. Am. Chem. Soc. 60 (1938), p. 309*

[3] *ISO 9277 (2008), Revision of first edition (ISO 9277:1995)]*

The new iSORB-HP for comprehensive pressure gas adsorption studies

The iSORB-HP is a series of state-of-the-art, bench top, automated, volumetric, high pressure gas sorption analyzers. The iSorb-HP is available as

- **iSORB-HP1** – 100 bar (1 port, max. 100 bar)
- **iSORB-HP1** – 200 bar (1 port, max. 200 bar)
- **iSORB-HP2** – 100 bar (2 ports, max. 100 bar)
- **iSORB-HP2** – 200 bar (2 ports, max. 200 bar)

The iSorb-HP (Figure 1) has been specially designed and constructed to provide reliable high pressure sorption data over a wide range of temperatures. Temperature control methods include a high-temperature mantle (standard), an optional recirculator system, an optional liquid nitrogen cryogenic system, and a cryocooler option. The materials of construction allow the iSorb-HP to work with hydrogen, methane, carbon dioxide, nitrogen, argon or any other non-corrosive gas. It can determine adsorption and desorption behavior of gases on any type of adsorbent such as activated carbon, zeolites, templated silicas, metal-organic frameworks, hydride formers, etc. Detailed equations of state are employed in the measurement software to ensure accuracy of data. In Figure 2 (right) the calculation of the results by use of different gas equations is demonstrated. The automatic measurement capabilities include:

Figure 1 *iSORB-HP1 and iSORB-HP2 for comprehensive high pressure gas adsorption studies*

- Sieverts style PCT isotherms
- Super-ambient temperature measurements (with appropriate temperature option)
- Sub-ambient temperature measurements (with appropriate temperature option)
- Cryogenic temperature measurements (with appropriate temperature option)
- Hydride formation/decomposition measurements as a function of temperature (requires hydride expansion option)

plus in-situ, software programmed sample degassing (no manual valve actuation, programmable ramp rate, target temperature, time under vacuum, backfill status (none - leave under vacuum, or backfill with helium).

Do not hesitate to contact **info@quantachrome.de** for further information about the method and the instrument and the possibility to use the high pressure gas adsorption as contract analyses in the LabSPA (Laboratory for Scientific Particle Analysis).

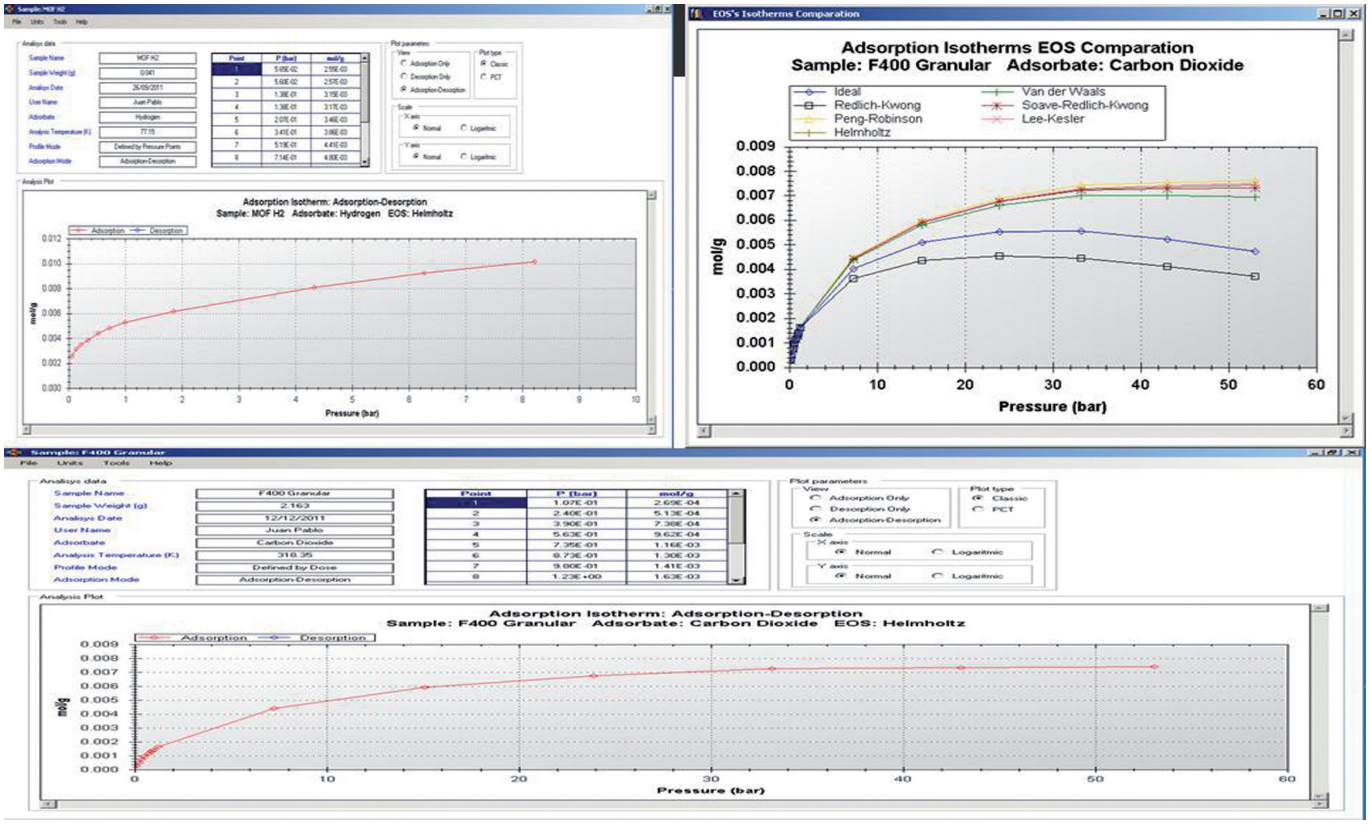

Figure 2 *Examples for high pressure gas adsorption, Hydrogen adsorption 77 K on MOF surface (left) and carbone dioxide adsorption at 45 °C (right, with calculation according different real gas equations)*

1 nm up to 10 cm

QUANTACHROME offers the ideal analytical instrument for almost all particle sizes

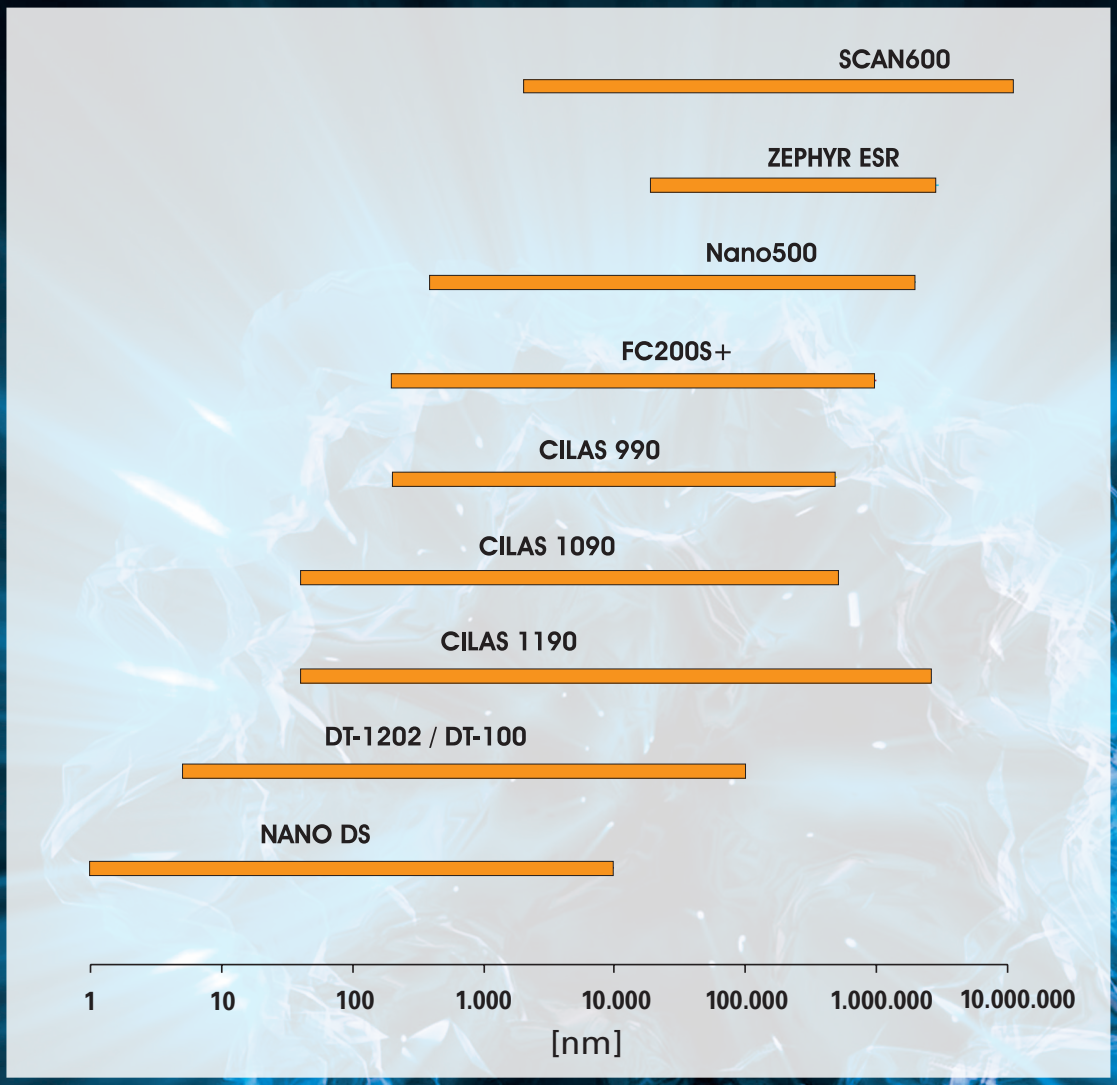

Quantachrome

Your partner in particle characterization

www.quantachrome.eu.com